J. Fluid Mech. (1996), vol. 326, pp. 285–319
Copyright © 1996 Cambridge University Press

Experiments on particle–turbulence interactions in the near-wall region of an open channel flow: implications for sediment transport

By Y. NIÑO AND M. H. GARCIA

Hydrosystems Laboratory, Department of Civil Engineering, University of Illinois at Urbana-Champaign, Urbana, IL 61801, USA

(Received 6 June 1995 and in revised form 3 June 1996)

A high-speed video system was used to study the interaction between sediment particles and turbulence in the wall region of an open channel flow with both smooth and transitionally rough beds. In smooth flows, particles immersed within the viscous sublayer were seen to accumulate along low-speed wall streaks; apparently due to the presence of quasi-streamwise vortices in the wall region. Larger particles did not tend to group along streaks, however their velocity was observed to respond to the streaky structure of the flow velocity in the wall region. In transitionally rough flows particle sorting was not observed. Coherent flow structures in the form of shear layers typically observed in the near-wall region interacted with sediment particles lying on the channel bottom, resulting in the particles being entrained into suspension. Although there has been some speculation that this process would not be effective in entraining particles totally immersed in the viscous sublayer, the results obtained demonstrate the opposite. The entrainment mechanism appears to be the same independent of the roughness condition of the bottom wall, smooth or transitionally rough. In the latter case, however, hiding effects tend to preclude the entrainment of particles with sizes finer than that of the roughness elements. The analysis of particle velocity during entrainment shows that the streamwise component tends to be much smaller than the local mean flow velocity, while the vertical component tends to be much larger than the local standard deviation of the vertical flow velocity fluctuations, which would indicate that such particles are responding to rather extreme flow ejection events.

1. Introduction

One of the most important engineering applications of the theory of turbulence arises from the fact that it plays an essential role in transport phenomena. Momentum, mass or heat transfer mechanisms are strongly related to turbulent processes. Turbulent diffusion of contaminants and heat transfer mechanisms have been investigated intensively; however the mechanics of sediment transport has yet to be thoroughly related to knowledge of turbulent processes. Instead, the transport of sediment has been traditionally described by empirical or semiempirical formulations, usually having limited general validity. Progress in the understanding of the physics underlying sediment transport mechanisms is related to parallel improvements in the knowledge of turbulence dynamics in open channel flows. In particular, since the interaction between flow and natural sediment occurs mainly in the vicinity of the

bed, detailed knowledge of the processes that govern the turbulence structure near the wall appears to be essential to advance a mechanistic approach to sediment transport phenomena.

It is currently well known that the streamwise velocity field in the near-wall region of a channel flow is organized into alternating narrow streaks of high- and low-speed fluid, which are quite persistent in time. Related to this spatial structure are intermittent, quasi-periodic events, consisting of outward ejections of low-speed fluid from the wall and inrushes of high-speed fluid toward the wall. Such near-wall events, which are associated with the so-called turbulent bursting, are largely responsible for the production and maintenance of turbulence in wall boundary layers (Robinson 1991).

It was probably Sutherland (1967) who first put forward the idea that a mechanism to entrain sediment grains into suspension would correspond to flow ejections associated with coherent structures in the near-bed region of a turbulent boundary layer. He speculated that turbulent eddies disrupt the viscous sublayer and impinge directly onto the sediment bed, such that the swirling motion of the fluid within the eddy would increase the local shear stress acting over individual grains, causing their acceleration, and eventually, due to the induced rolling motion and depending on their relative height above the mean bed level, such grains would leave the bed. Although Sutherland's idea of eddies coming from above and impinging on the bed may not be totally correct in the light of the present knowledge about the turbulence structure in the wall region of boundary layer flows, it delineates the basic turbulence–particle interaction that results in particle entrainment, which has been verified more recently by empirical evidence.

In fact, based on field observations, Jackson (1976) analysed the implications of the bursting phenomenon on the mechanics of sediment transport in alluvial channels, and related such phenomenon to the sediment-laden kolks and boils observed on the free surface of rivers. Likewise, different experiments have been conducted to visualize the flow field in the wall region of turbulent boundary layers with the aim of inferring the mechanism by which particles are entrained into suspension (e.g. Grass 1974; Sumer & Oguz 1978; Sumer & Deigaard 1981; Ashida & Fujita 1986; Yung, Merry, & Bott 1988; Rashidi, Hetsroni, & Banerjee 1990; Best 1992; Kaftori, Hetsroni, & Banerjee 1995*a*, *b*). Kaftori *et al*. propose a funnel type of vortex as the dominant coherent structure in such region. They conclude that coherent structures are the main factor affecting particle motion near a solid boundary in turbulent flows. Nevertheless, it is important to point out that Kaftori *et al*.'s results, as well as those of most of other experimental studies, correspond to almost neutrally buoyant particles of rather large sizes, which may exhibit a behaviour different to that of much heavier, albeit smaller, natural sand particles. Although Grass (1974) did utilize natural sediment in his experiments, unfortunately he does not provide enough details about the experiments nor presents sufficient or conclusive data. In conclusion, to date, few precise descriptions of the particle–turbulence interactions responsible for the transport of sediment in the wall region of an open channel flow seem to exist.

Herein some experimental results regarding particle–turbulence interactions in the near-wall region of a turbulent open channel flow are presented, including particle interactions with wall streaks and the phenomenon of particle entrainment into suspension. The motion of particles lying over a smooth boundary as well as over a rough bed is investigated using both particle–flow visualization and particle tracking techniques. These experimental results differ from others in that heavy, although small, natural sand particles are observed to interact with the turbulence of the flow,

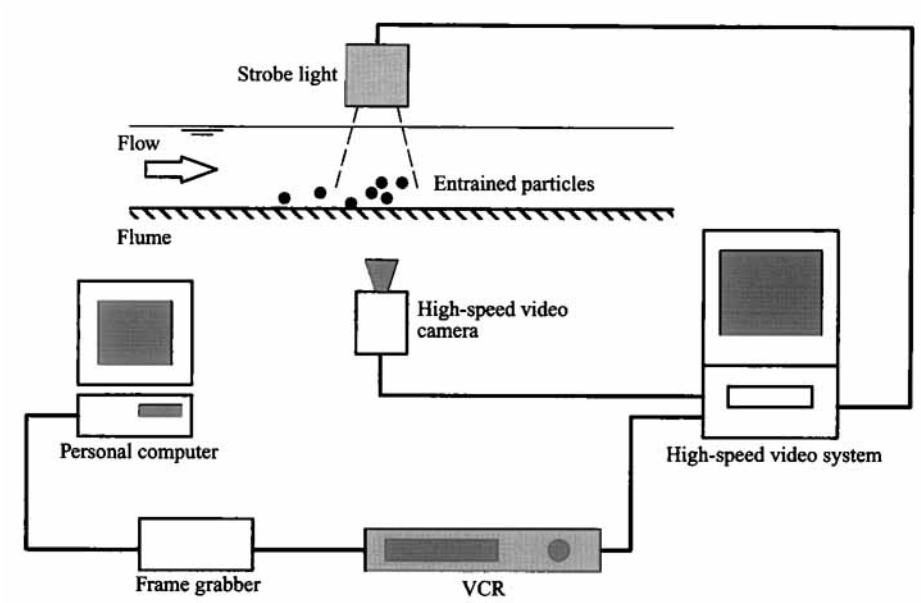

FIGURE 1. Schematic view of experimental set-up.

as opposed to the light (almost neutrally buoyant), larger particles that have been used in previous studies. Also, the present investigation concentrates solely on the processes occurring in the wall layer of open channel flows, as opposed to other studies that analyse almost the whole flow field, thus having a better resolution of particle motion during the initial stages of particle entrainment.

2. Experiments

2.1. *Experimental set-up*

The experiments were conducted in a rectangular open channel 18.6 m long, 0.30 m wide, and 0.28 m high, with a slope set to a value of about 0.0009. The test section was located 12 m downstream from the entrance. A high-speed video system, Kodak Ektapro TR Motion Analyzer, which has the capability to record up to 1000 frames per second, was used to record particle motion. The solid-state sensor of this system has a pixel array structure of 240 columns and 192 rows. A strobe light with a flash-duration of 20 μs was synchronized with the high-speed video system to provide whole-field illumination. The video images acquired were downloaded from special high-speed Kodak tapes onto standard VHS tapes, and then digitized into a personal computer using a frame grabber. The images were analysed using the National Institute of Health's *Image* public domain software. A schematic view of the experimental set-up is shown in figure 1.

2.2. *Experimental method*

The experiments were carried out under uniform flow conditions. Particles were fed externally to the flow at a distance sufficiently far upstream from the observation window to ensure particle motion reached independence from initial conditions before going into the field of view of the camera. Particle motion was recorded from the side, through the observation window, and in some cases also from the

top, using the high-speed video system set at a recording rate of 250 frames per second (f.p.s.). In the case of side views, typical dimensions of the flow field registered by the camera were about 1 to 2 cm in the streamwise direction by about 0.8 to 1.5 cm in the vertical direction. This corresponded to flow fields of about 200 by 150 wall units to about 550 by 400 wall units, where wall units denote the length scale ν/u_*, with ν denoting kinematic viscosity and u_* denoting the flow shear velocity. These dimensions were found adequate to resolve spatially individual particles (since they corresponded to an area of at least 25 pixels on the digitized video images) as well as particle trajectories during entrainment. Likewise, the recording rate of 250 f.p.s. was found to provide an adequate temporal resolution of the particle trajectories. It is important to note that a recording rate of 250 f.p.s. is about 8.3 times faster than that of regular video. On the other hand, the depth of field provided by the camera lenses was about 1 mm which was large enough to allow particles to remain within the field of view of the camera during entrainment.

A number of experiments were carried out in which a solution of white clay in water was injected through an orifice in the channel bottom to act as a marker for flow structures developing at the wall. The tracer discharge was controlled so as to minimize disturbance of the flow, and to allow the tracer to move along the bed before flow ejections lifted filaments away from the channel bottom. This technique allows one to visualize the interaction between particles and flow ejections however it does not provide information about the flow structure in the region above the ejection, nor is it efficient in marking sweeps events.

2.3. *Experimental conditions*

Two different series of experiments (S and T) were conducted corresponding to two different surface roughness. The first series of experiments (Series S) corresponded to a channel with smooth walls. The second series (Series T) corresponded to a channel with bottom roughness in the transitionally rough regime. The bottom roughness in this case was of the k-type (Perry, Schofield & Joubert 1969; Perry & Li 1990), and was created by glueing sand particles with a mean size of about 0.53 mm to the originally smooth surface of the channel bottom.

Flow depths used in both series of experiments covered a range from about 2.5 to about 6 cm. Flow conditions corresponded to values of the Reynolds number (defined as $Re = Uh/\nu$, where U denotes flow mean velocity, and h denotes flow depth) in the range from about 5000 to about 30000, and to values of the Froude number (defined as $Fr = U/(gh)^{1/2}$, where g denotes gravitational acceleration) of about 0.5 to 0.6, which corresponded to subcritical flows. Values of the flow shear velocity, u_*, estimated for each experimental condition by means of a best fit of velocity measurements made with a hot-film probe to the logarithmic velocity distribution (Niño 1995), were in the range from 0.015 m s^{-1} to about 0.040 m s^{-1}.

Five different particles were used in the experiments for both series S and T, namely glass beads with mean diameter, d_p, of 38 and 94 μm, and natural sand particles with d_p values of 112, 224, and 530 μm, respectively. All the particles had a submerged specific density, $R = (\rho_s - \rho)/\rho$, of about 1.65, where ρ_s denotes the particle density, and ρ denotes the fluid density. A summary of the particle characteristics is presented in table 1, including the particle dimensionless diameter $R_p = (g R d_p^3)^{1/2}/\nu$, and the particle settling velocity, v_s, which was estimated theoretically assuming the particles were spheres with a diameter equivalent to d_p. In the experiments of Series T the size of the particles transported by the flow, d_p, was different from the size of the particles

d_p (mm)	R_p	v_s (cm s^{-1})	d_p/d_b
38	0.9	0.13	0.072
94	3.7	0.70	0.177
112	4.8	0.96	0.211
224	13.5	3.00	0.423
530	49.1	8.91	1.000

TABLE 1. Particle properties

Series	h (m)	u_* (m s^{-1})	Re	Re_*	Re_{p*}	τ_*
S	0.033	0.019	10760	627	4.3	0.100
	0.039	0.021	14470	803	4.6	0.117
	0.045	0.022	18650	995	5.0	0.135
	0.050	0.023	22500	1165	5.2	0.150
T	0.047	0.030	18840	1436	6.8	0.255
	0.051	0.032	21480	1634	7.2	0.284
	0.056	0.035	25240	1924	7.7	0.329

TABLE 2. Experimental conditions of experiments aimed at characterizing particle entrainment into suspension

forming the bed roughness elements, d_b. Values of the ratio d_p/d_b in the experiments of Series T are also shown in table 1.

In Series S, values of the particle Reynolds number, $Re_{p*} = u_* d_p/\nu$, were in the range from 0.70 to about 20, which indicates that in some of these experiments particles had sizes smaller than the corresponding thickness of the viscous sublayer (estimated as $5\nu/u_*$).

Experimental conditions corresponding to those experiments aimed at analysing characteristics of particle entrainment into suspension are presented in table 2, including values of the dimensionless Shields shear stress defined as $\tau_* = u_*^2/(g\,R\,d_p)$.

3. Method of analysis

The video recordings of particle entrainment and particle–flow interactions were analysed in order to elucidate the physical mechanisms involved in such phenomena. Selected frames of the video recordings were digitized into a personal computer. Images were analysed in order to obtain the position of particles in successive frames. This was done manually in most of the cases, although an automatic particle tracking algorithm (Dill 1994; Hassan *et al.* 1992) was used in some cases. In general, all particles appearing in the frames were tracked, up to a maximum number of about 100 particles for each experiment, so no specific sampling method was used in the analysis. From the digitized particle trajectories, kinematic and dynamic characteristics of particle motion during entrainment into suspension could be obtained. This information complemented the visualizations of flow–particle interactions and helped to develop a conceptual model of the mechanics of particle entrainment into suspension.

In what follows x, y, and z denote coordinates in the streamwise, vertical and transverse directions, respectively. Also, wall units denote characteristics scales formed using u_* and ν as variables, such that for example ν/u_* represents a length scale,

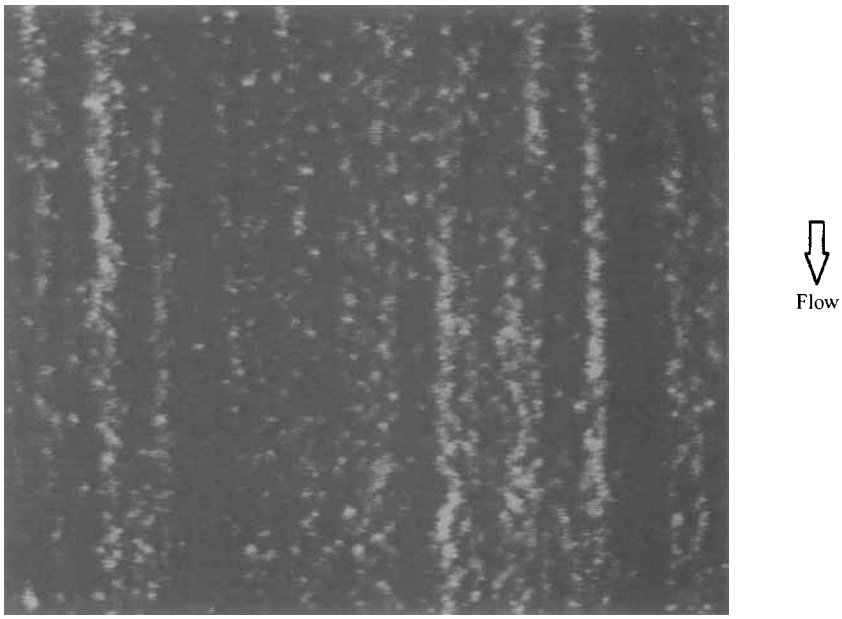

FIGURE 2. Glass beads moving along low-speed streaks. Field of view is about 900 by 1000 wall units. Experimental conditions correspond to $Re = 9000$, $d_p = 94$ μm, $Re_{p*} = 1.7$.

u_* represents a velocity scale, and ν/u_*^2 represents a time scale. Variables with the subindex + have been made dimensionless with wall units.

4. Particle motion in the plane (x, z)

4.1. *Experiments of Series S: smooth flows*

Flow visualizations of particles moving along the channel bottom in experiments of Series S, corresponding to smooth flows, showed that particles immersed within the viscous sublayer tend to be sorted in the spanwise direction, such that they accumulate along low-speed streaks of the flow. This is a well-recognized phenomenon observed among others, by Grass (1971), Schmid (1985), Yung *et al.* (1989), Rashidi *et al.* (1990), and Kaftori *et al.* (1995*a*, *b*). An example of the typical situation observed from plan views of the flow is shown in figure 2, which corresponds to the experimental conditions $Re = 9000$, $d_p = 94$ μm, $Re_{p*} = 1.7$. Therein, lighter zones are regions where particles accumulate, marking elongated strips corresponding to low-speed streaks, while darker zones are regions with a much lower concentration of particles, which correspond to high-speed streaks.

The low-speed streaks marked by the particles moving along the bed appear to have lengths on the order of about 1000 to 2000 wall units. Average measured values of the dimensionless transverse spacing of the streaks, λ_+, as observed in the present experiments are equal to about 100 for the range of values of Re covered herein, which is accepted as universal for the spacing of wall streaks in turbulent boundary layers (Robinson 1991). This seems to indicate that the presence of particles in the viscous sublayer has a negligible effect on the spacing of the streaks, which is in complete agreement with the results of Rashidi *et al.* (1990) (see also Hetsroni 1991). These researchers varied the loading of particles in the wall region of a channel

flow and observed the effect of the presence of the particles on the streaks marked by hydrogen bubbles, concluding that although the presence of the particles seems to influence the frequency of wall ejections, it has a negligible effect on the streaks appearance and their spacing.

Rashidi *et al.* (1990) concluded that the presence of particles in the wall layer tends to increase the frequency of occurrence of wall ejections for particles of sizes somewhat larger than the thickness of the viscous sublayer (values of Re_{p*} larger than about 5 to 10), and to decrease such frequency for smaller particles. In the case of large particles Rashidi *et al.* conclude that the increase in the frequency of wall ejections would indicate that the particles have a destabilizing effect on the coherent structures of the flow in the wall layer. Analogously, it can be concluded that particles totally immersed in the viscous sublayer would have a stabilizing effect manifested in the reduction of the frequency of ejections. Indeed, the present observations indicate that such particles do have a stabilizing effect on the turbulence structure of the viscous sublayer, in that the streaks marked by them are very persistent in time and do not exhibit the strong wavering and lateral oscillations observed in flow visualizations without particles (e.g. Kline *et al.* 1967). In fact, according to Blackwelder (1988) the persistence of the streaks in flows without particles would be on average about 480 wall time units with some streaks persisting up to 2500 wall time units. The streaks observed herein had persistences roughly 2 to 3 times longer. It can be speculated that the stabilizing effect of the small particles would be related to the extra dissipation of energy associated with friction between fluid and particles, while the destabilizing effect of larger particles would be associated with the presence of wakes and direct interaction of the particles with flow structures. For instance Hetsroni (1991) explains the increase in the frequency of wall ejections observed in the experiments of Rashidi *et al.* (1990) in the presence of particles protruding over the viscous sublayer as a consequence of the direct interaction between vortex filaments and particles, such that the former would get attached to the moving particle instead of to the bottom wall, which would create a premature detachment of the vortex structure from the wall, and thus a premature ejection.

Extended persistence of streaks marked by particles is also probably due to the sheltering and increased resistance to movement induced by the close particle grouping. This, as discussed by Kaftori *et al.* (1995*a*), would imply that only the more violent inrush/sweep events can break up the particle accumulation. Also the particle streaks may tend to fix vortical structures and their streamwise trailing legs (responsible for streak formation) at particular spanwise locations for extended time periods.

Some measurements were made, as part of the present study, of the trajectories and velocities of particles moving along low- and high-speed streaks. In general, particles completely immersed within the viscous sublayer moving along low-speed streaks have streamwise velocities on the order of 60% to 70% of the mean flow velocity, estimated using the law of the wall, $u_+ = y_+$, at an elevation equal to the particle radius. Identical particles moving along high-speed streaks have streamwise velocities on the order of about 1.5 to 2.0 times the mean flow velocity at an elevation equal to the particle radius, although in this case the particle velocity has much more variability than in the former. This is illustrated in figure 3, where the behaviour of eight different particles tracked in one of the experiments of Series S for the conditions $Re = 9000$, $d_p = 94$ μm, $Re_{p*} = 1.7$, has been plotted in the phase space $(z_+, u_p/u_{fp})$, where u_p denotes the instantaneous streamwise particle velocity, and u_{fp} denotes the mean velocity of the flow at an elevation equal to the particle radius, such that four of them move along a low-speed streak and the other four move along a high-speed

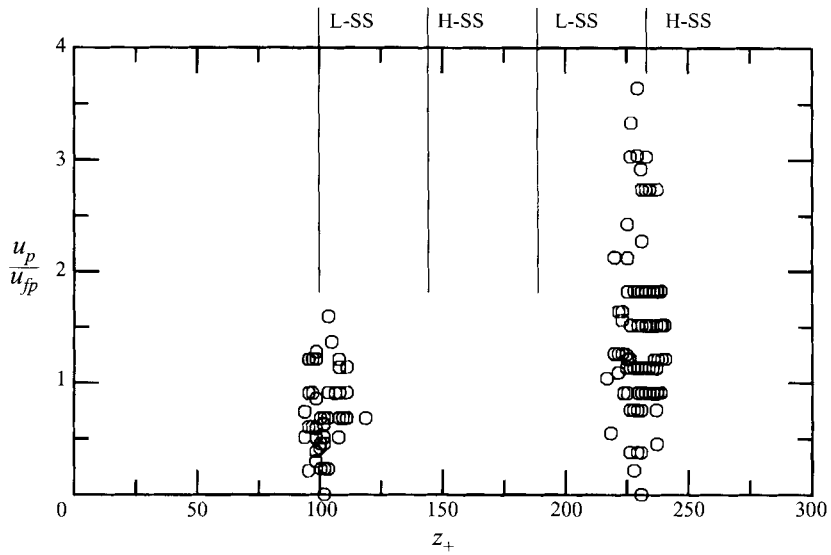

FIGURE 3. Instantaneous streamwise particle velocities along wall streaks. Experiments of Series S, Re = 9000, d_p = 94 μm, Re_{p*} = 1.7. In the legend H-SS denotes high-speed streak, and L-SS denotes low-speed streak.

streak. As seen therein, those particles moving along the low-speed streak have values of u_p/u_{fp} generally lower than unity, with an average of about 0.7, and a standard deviation of about 0.3. On the other hand, those particles moving along high-speed streaks have values of u_p/u_{fp} as high as 3.5, although the average is about 1.5 with a standard deviation of about 0.8. Clearly the particle velocity along the high-speed streak exhibits much more variability in time, which would be a consequence of higher turbulent intensities prevailing in those regions of the viscous sublayer.

The present observations indicate that particles are picked up from low-speed streaks, lifted away from the wall by some kind of ejection events, and deposited back to the bed along the high-speed streaks. This is in complete agreement with observations by Sumer & Oguz (1978), Sumer & Deigaard (1981), Rashidi *et al.* (1990) and Kaftori *et al.* (1995*a*) on the entrainment into suspension of almost neutrally buoyant particles. Once the particles get deposited along the high-speed streaks, they tend to be displaced toward the low-speed streaks by the action of transverse flows related to longitudinal vorticity. This coincides with observations on the formation of streaks using fine sand made by Grass (1971). According to him, the fast transverse displacement of particles from the margins of the high-speed streaks toward the low-speed streaks would be indicative of the existence of strong inrushes of high-momentum fluid toward the wall.

An interesting result of the present observations is that particles of sizes larger than the thickness of the viscous sublayer do not tend to be sorted along the wall streaks, that is, they do not tend to accumulate along the low-speed streaks, although groups of particles located in certain regions along the bottom wall do seem to exhibit sudden accelerations, apparently as a consequence of the occurrence of inrush events associated with the existence of high-speed streaks. This observation indicates that the formation of wall streaks is a phenomenon related to the structure of the turbulence within the viscous sublayer, which appears to be confined within elevations lower than about 5 wall units from the bottom wall, such that it is not effective in inducing

the grouping of particles protruding somewhat over the viscous sublayer, although it is apparent that it can still influence their velocity. This is in agreement with Kline *et al.*'s (1967) flow visualizations using hydrogen bubbles, which indicate that the streaks tend to become less noticeable and eventually to vanish at distances from the bed larger than about 5 wall units.

It is necessary to mention, however, that direct numerical simulations of wall-bounded turbulent flows show the existence of streaks at values of y_+ as large as about 10 (Moin & Kim 1982; Moin & Spalart 1989). According to the flow visualizations of Smith & Schwartz (1983), low-speed streaks appear as well-organized and very persistent structures only for values of y_+ up to about 5. At higher values of y_+ the low-speed regions are still recognizable, although they exhibit strong but intermittent outward motion combined with spanwise rotation, which make flow patterns more irregular as they evolve in time. Smith & Schwartz conclude that the most energetic and regular rotational behaviour occurs in a region corresponding to values of y_+ lower than about 25, and that this rotational behaviour suggest the presence of counter-rotating streamwise vortices which would be related to low-speed streak formation.

From the above discussion it appears that the formation of low-speed streaks is related to the presence of counter-rotating, streamwise vortices, extending distances up to about 25 wall units from the channel bottom. It seems plausible that cross-flows resulting from the streamwise structures would be more persistent and well organized within the viscous sublayer, which may explain why they are more effective in pushing particles with their centroid located well within the viscous sublayer toward the low-speed regions, rather than larger particles protruding from the sublayer. Also, it must be considered that larger particles have more inertia than smaller ones and therefore they are less responsive to flow velocity fluctuations such as those associated with the cross-flows.

A similar result was obtained by Kaftori *et al.* (1995*a*), who also found that the tendency of particles to aglomerate into streaks is due to the presence of streamwise vortices, which they propose to have a funnel shape, and is a function of particle size, such that particles of sizes similar to that of the viscous sublayer tend to form streaks more than larger or smaller ones.

Pedinotti, Mariotti & Banerjee (1992) performed a direct numerical simulation of particle behaviour in the wall region of a turbulent channel flow. They found that particles with very low specific density, $R = 0.03$, tend to be grouped along low-speed streaks; however the degree of sorting appears to depend on the particle dimensionless time constant (a measure of the particle inertia), defined as $t_{p+} = (\rho_s d_p^2 u_*^2)/(18 \nu^2 \rho)$, such that maximum sorting is obtained for values of t_{p+} of about 3. For smaller values of t_{p+}, the particles tend to get distributed uniformly along the bed, and the same happens for larger values of t_{p+}. Pedinotti *et al.* point out that the sorting mechanism would be due to the presence of a rotation motion in the high-speed regions which pushes the particles out of them. They speculate that this mechanism would be effective in grouping particles along the viscous sublayer as long as their time constant is small enough to follow the streak motion, but not so small as to be sensitive to high-frequency fluctuations, which would tend to distribute the particles uniformly.

In the present experiments particle grouping along low-speed streaks was observed for values of t_{p+} in the range from about 0.05 to about 4. On other hand, particles protruding from the viscous sublayer, which do not tend to group along the wall streaks, have values of t_{p+} larger than 10. These results are only in partial agreement

with the numerical simulations of Pedinotti *et al.*, since according to their results sorting would be much less conspicuous than observed herein for values of t_{p+} lower than say 1. Nevertheless, the present results agree, at least qualitatively, with them in that particles with large time constants do not tend to group along wall streaks.

4.2. *Experiments of Series T: transitionally rough flows*

Observations of the video recordings made in the experiments of Series T, corresponding to transitionally rough flows, indicate that in this situation the formation of streaks is much less evident than in the case of smooth flows. In fact, it seems that the roughness elements, with sizes of about 10 wall units, totally disrupt the structure of the viscous sublayer as compared with the smooth bed situation. Particles with sizes smaller than about 1/5 of the size of the roughness elements were observed to move within the interstices of the latter, and therefore their path was imposed mainly by the random distribution of bed obstacles. Larger particles were observed to move over the roughness elements, at distances well above 5 wall units from the bottom wall, and did not show any tendency to group together along preferential lines.

The above observations are in total agreement with those by Sumer & Deigaard (1981). According to them, in the case of a smooth wall, inrushes of high-speed fluid hit the bottom and spread out sideways; the lateral flows of fluid along the neighbouring sides of two such adjacent high-speed zones of fluid run together, merge with each other and are retarded, which in turn gives rise to a low-speed wall streak. In the case of a rough wall, the lateral flows of fluid along the neighbouring sides of two adjacent high-speed zones are likely to be retarded by form drag of the roughness elements, which cause the fluid to be trapped between the protrusions, leading to longitudinal localization of the low-momentum fluid and thus causing the disappearance of the smooth-boundary wall streaks. Indeed, Grass (1971) reported that the long twisting streamwise vortices, very apparent close to the smooth boundary during inrush–ejection cycles, were much less evident in the transitional and rough boundary flows in his tests, which would imply that low-speed wall streaks cease to exist in the case of a rough wall.

Nevertheless, new experimental evidence presented by Grass, Stuart & Mansour-Tehrani (1991) seems to indicate that wall streaks would continue to exist in the transitionally rough and rough flow regimes, although their characteristics would tend to change as the bed roughness is increased. In general, Grass *et al.* point out that the spacing of the streaks tends to increase with the bed roughness, while their streamwise coherence is substantially reduced. On the other hand, it is also apparent that the effect of the wall streaks is felt only in a region adjacent to the roughness elements, which has a rather reduced vertical extent.

Although the wall streaks would persist in transitionally rough flows like those of Series T according to the previous discussion, it also appears that those streaks do not have the strong coherence, persistence, and vertical extent observed in the case of smooth flows. This implies that they are not strong enough to induce heavy sediment particles to sort along them, which is in agreement with the present observations. As was already mentioned, those sand particles that were large enough as to move over the roughness elements in the present experiments did not show any tendency to sort along preferential lines. Depending on flow conditions they were observed either saltating along the bed or being entrained into suspension by the turbulence of the flow as discussed in the next section.

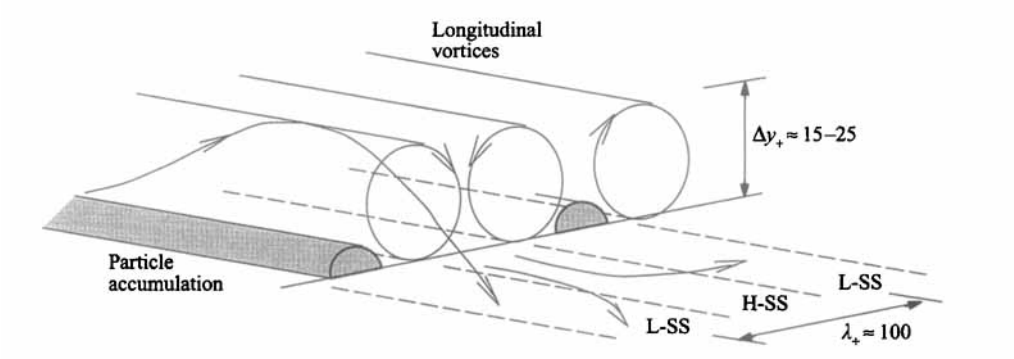

FIGURE 4. Conceptual model of streak formation.

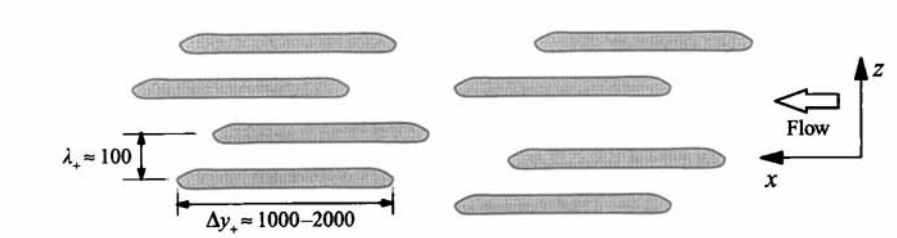

FIGURE 5. Low-speed streaks, zones of particle accumulation. After Hetsroni (1991).

4.3. *Discussion and conceptualization*

The evidence presented so far allows a few general conclusions with respect to the motion of particles in the (x, z)-plane along the bottom wall of a turbulent channel flow and their interaction with wall streaks. In the first place the wall streaks in a smooth flow appear to be related to the presence of counter-rotating streamwise vortices. These would extend about 1000 to 2000 wall units in the streamwise direction, and about 15 to 25 wall units from the bottom in the vertical direction, although they appear to lose their coherence outside the viscous sublayer. The spanwise dimension of the longitudinal vortices would be lower than about 50 wall units so the total spanwise extent of the counter-rotating pair would be about 100 wall units, which corresponds to the spacing between low-speed streaks. These vortices would create a 'pumping' effect which produces ejections of low-momentum fluid away from the wall on one side of the vortex core, and inrushes of high-momentum fluid toward the wall on the other (Robinson 1990). The inrushes of high-momentum fluid would impinge against the wall and create strong cross-flows toward the low-speed regions. These cross-flows would be most responsible for pushing particles toward and their accumulation in the low-speed regions (figure 4). Since the cross-flows are stronger and more coherent close to the bed they would be most effective in pushing particles totally immersed within the viscous sublayer, rather than particles protruding from it, such that the latter do not tend to accumulate along wall streaks.

Groups of 3 to 5 counter-rotating pairs of streamwise vortices emerge and collapse quasi-periodically in time, and distribute rather randomly along the bed (figure 5). The persistence of the structures in the absence of particles is on average about 500 wall time units, and increases about 2 to 3 times in the presence of particles. This would indicate that the particles have a stabilizing effect on the structures of the flow; however this would be true for small particles only (smaller than say the thickness of the viscous sublayer), such that larger particles would have a destabilizing effect over

such structures. The spacing of the streaks, on the other hand, is not affected by the presence of particles.

In the case of a rough boundary, the roughness elements disrupt the structure of the viscous sublayer, and although the wall streaks would persist in these conditions, they would lose coherence, persistence and spatial extent. This, however, does not affect the mechanism that generates ejections of low-speed fluid away from the wall, and inrushes of high-speed fluid toward the wall. Cross-flows resulting from inrushes are likely to be retarded by form drag of the roughness elements, which would cause the fluid to be trapped between the protrusions, leading to longitudinal localization of low-momentum fluid. Particles of small size compared to the roughness elements (with sizes of about 1/5 of those of the roughness elements) tend to move within the interstices of the latter, and therefore their path is controlled mainly by the random distribution of bed protrusions. Larger particles move over the roughness elements and do not tend to accumulate along specific regions of the flow.

5. Particle motion in the plane (x, y)

5.1. *Experiments of Series S: smooth flows*

5.1.1. *Results from visualizations of flow and particle motion*

As already discussed, visualizations of particle motion in the near-bed region of the smooth flows of Series S showed that particles tend to be picked up from low-speed streaks, lifted away from the wall by some kind of ejection mechanism, and deposited back to the bed along the high-speed streaks, from where they tend to be displaced toward the low-speed streaks by the action of cross-flows related to longitudinal vorticity.

There exists a consensus, based primarily on experimental evidence, that the mechanism that causes the ejection of the particles away from the bed is related to interactions between the particles and intermittent events associated with the phenomenon of turbulent bursting, during which low-momentum fluid is ejected toward the outer regions of the wall layer (Grass 1974; Sumer & Oguz 1978; Sumer & Deigaard 1981; Ashida & Fujita 1986; Yung *et al.* 1989; Rashidi *et al.* 1990; Kaftori *et al.* 1995*a*, *b*). The same conclusion is reached by Pedinotti *et al.* (1992) whose direct numerical simulations of particle–turbulence interactions in the near-wall region of a channel flow have shown that particles are lifted from the bed by the action of upflows caused by quasi-streamwise vortices which detach low-speed fluid from the wall.

Results of flow visualizations carried out in the present investigation have shown that low-speed streaks tend to be lifted-up as a consequence of quasi-periodic ejections of low-momentum fluid away from the channel bottom, and to evolve into some kind of flow coherent structure. The most frequently observed coherent structures correspond to inclined, thin shear layers of concentrated spanwise vorticity, similar to those revealed by the analysis of data bases generated through Direct Numerical Simulations (DNS) (e.g., Jimenez *et al.* 1988; Guezennec, Piomelli & Kim 1989), and those observed experimentally using Particle Image Velocimetry (PIV) (e.g. Liu *et al.* 1991; Urushihara, Meinhart & Adrian 1993). The shear layers observed herein have a shape which appears to be invariant with the Reynolds number when plotted in wall units. These structures were observed to maintain their identity for as long as 60 to 80 wall time units, to extend vertically a distance of about 100 wall units with a mean inclination angle to the bed of about 14°, and to have convection

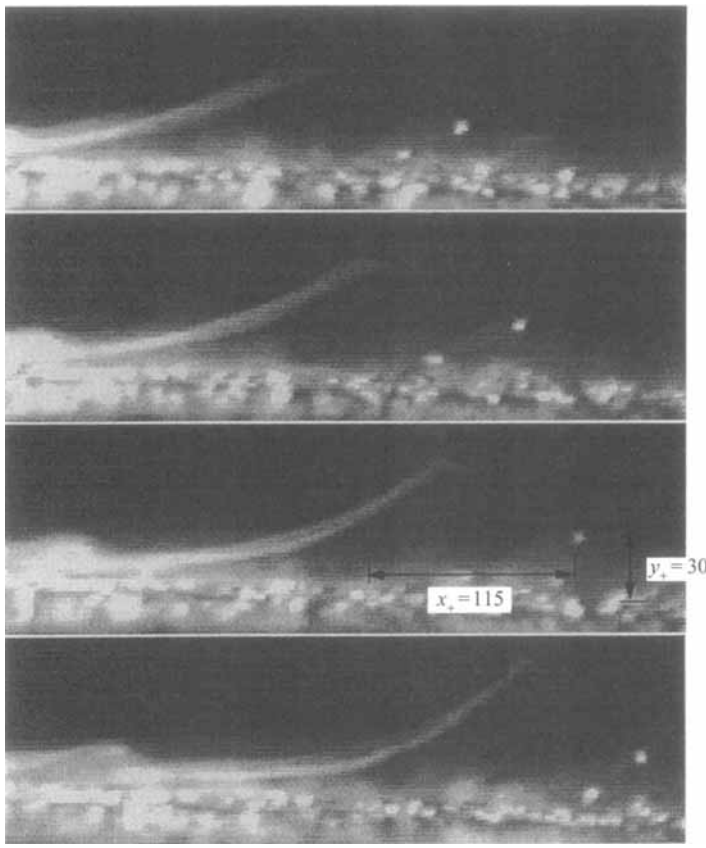

FIGURE 6. Sequence of images of particle–shear layer interaction. Experiments of Series S, $Re = 15\,000$, $d_p = 224$ μm, $Re_{p*} = 4.5$. Field of view of each image is about 375 by 114 wall units, and the time interval between images is 0.008 s. The shear layer is marked using a solution of white clay in water injected through the bottom of the channel.

velocities of about 10 wall units and frequencies of occurrence of about 0.003 wall units. Typically, at distances of about 100 to 200 wall units downstream from the structure a negative peak of the streamwise velocity fluctuations was measured (see García, López & Niño 1995), which appears to travel with the structure, and which would be correlated with positive vertical velocities of the flow in what would be an ejection event of low-momentum fluid away from the wall.

The present results indicate that the shear layers described above interact with particles lying on the bed, such that the flow ejection occurring downstream of the structure would induce the lift-up of particles away from the bed. This is illustrated in figure 6, where a sequence of images of an inclined shear layer being convected and stretched in the streamwise direction is shown, together with a sand particle which is being lifted-up from the bed at a distance of about 115 wall units downstream of the structure, apparently responding to an ejection event taking place in such region. The experimental conditions correspond to $Re = 15\,000$, $d_p = 224$ μm, $Re_{p*} = 4.5$, and the time interval between images is 0.008 s.

The present observations indicate that particle streamwise velocities during ejections are somewhat smaller than the convection velocity of the shear layers. This means that, as time goes by, shear layers and ejected particles tend to get closer together

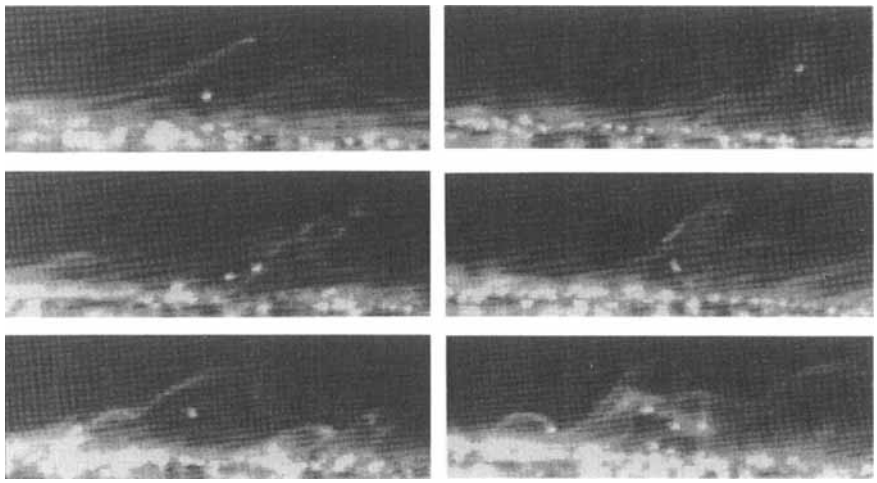

FIGURE 7. Different degrees of particle–shear layer interaction. Experiments of Series S, $Re = 15\,750$, $d_p = 224$ μm, $Re_{p*} = 4.7$. Field of view of each image is about 307 by 105 wall units.

and to have a more direct interaction, as is illustrated in figure 7, where different images show different degrees of interaction between particles and shear layers. As seen therein particles tend to get closer to the shear layers and eventually they get trapped within the flow field associated with the structures. In some some cases it was observed that particles lined-up along the shear layer and followed its path as the structure was stretched toward the outer regions of the wall layer. In some other cases the particles lost correlation with the shear layer and were observed to lag behind it until they were either deposited back on the bed, or taken-up by a new developing flow ejection.

To illustrate the above point, figure 8 shows a conceptualization of the relative motion of an ejected particle with respect to the shear layer. That is, it schematizes the particle motion as seen from a system of reference moving with the convection velocity of the flow structure. In that figure, the relative flow velocity field around the shear layer is also sketched, based on the experimental measurements using PIV by Urushihara *et al.* (1993). According to those observations, there appears to be a relative stagnation point located over the shear layer which corresponds to a saddle point of the relative velocity vector field. The zone downstream from the structure corresponds to a low-velocity region where the relative flow field is in the upstream direction toward the shear layer. The zone upstream from the structure corresponds to a high-velocity region where the relative flow is in the downstream direction, also toward the shear layer. Along the shear layer, the relative velocity vectors are in the direction of the inclined structure and have a larger magnitude upstream from the structure than downstream from it, so the shear layer represents a zone of concentrated transverse vorticity. The initial ejection of the particle would take place at a distance of about 100 to 200 wall units downstream from the structure and the relative motion of the particle would be in the upstream direction toward the shear layer. Afterwards the particle may either interact directly with the shear layer or lose correlation with it as discussed previously.

It is important to point out that the observed flow ejection events were not always effective in entraining the heavy particles tested herein into suspension. In fact, an analysis of the threshold conditions for particle entrainment into suspension (Niño

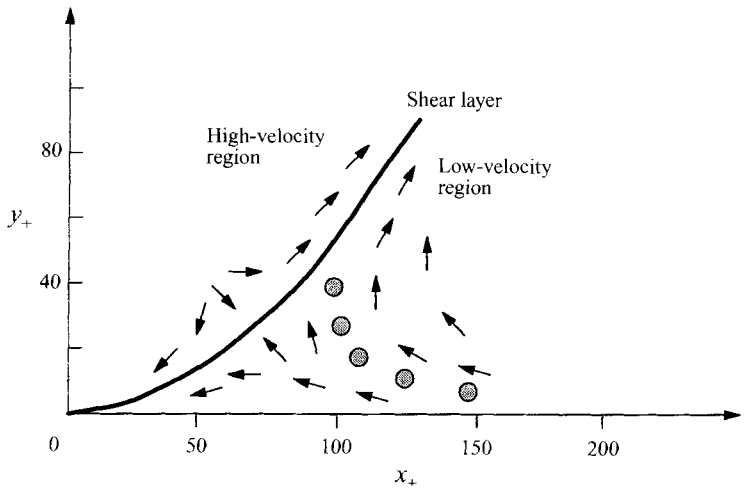

FIGURE 8. Schematic view of particle motion as seen from a system of reference moving with the shear layer. Circles represent different relative positions of the particle as it is ejected away from the bed. Arrows sketch the relative flow velocity field surrounding the shear layer as measured by Urushihara *et al.* (1993).

1995; Niño and García 1995) has shown that as the particle size gets smaller than the thickness of the viscous sublayer, progressively higher values of the bed shear stress are required to entrain the particle into suspension (for instance, the threshold value of the shear velocity for particle entrainment into suspension was found to be inversely proportional to the 0.15 power of particle diameter). This suggests that the relative intensity of the ejection events gets weaker as the bottom wall is approached. Indeed, according to Bark (1975), values of the Reynolds stress, $\overline{u'v'}$, during flow ejection events would have the following dependence on y_+:

$$-\overline{u'v'}/u_*^2 = c_1 y_+^3 \exp(-c_2 y_+^2) \tag{5.1}$$

where the constants c_1 and c_2 can be obtained by adjusting (5.1) to the measurements by Kim, Kline & Reynolds (1971), which gives the values 1.87×10^{-3} and 4.42×10^{-3}, respectively. Clearly (5.1) indicates that the intensity of the ejection events scales with u_*^2, or equivalently with the bed shear stress. That is, the intensity of the ejection events at constant value of y_+ can be expected to increase as the bed shear stress increases. Equation (5.1) is plotted in figure 9 together with the experimental values measured by Kim *et al.* As seen therein the maximum value of the shear stress occurs outside the viscous sublayer, at a distance from the bed slightly less than 20 wall units. Inside the viscous sublayer, the intensity of the shear stress due to the flow ejection decreases sharply toward the bed.

With respect to the previous discussion, it is necessary to mention that Sumer & Oguz (1978), and Yung *et al.* (1989), studying the entrainment into suspension of particles with very small submerged specific density concluded that flow ejection events have a negligible effect in entraining particles totally immersed within the viscous sublayer. The present results contradict this conclusion, as is evident from the visualizations shown in figures 6 and 7, all corresponding to heavy particles of sizes smaller than the thickness of the viscous sublayer, which indicate that bed shear stresses in Sumer & Oguz's, and Yung *et al.*'s experiments were not sufficiently high to cause the entrainment of such particles.

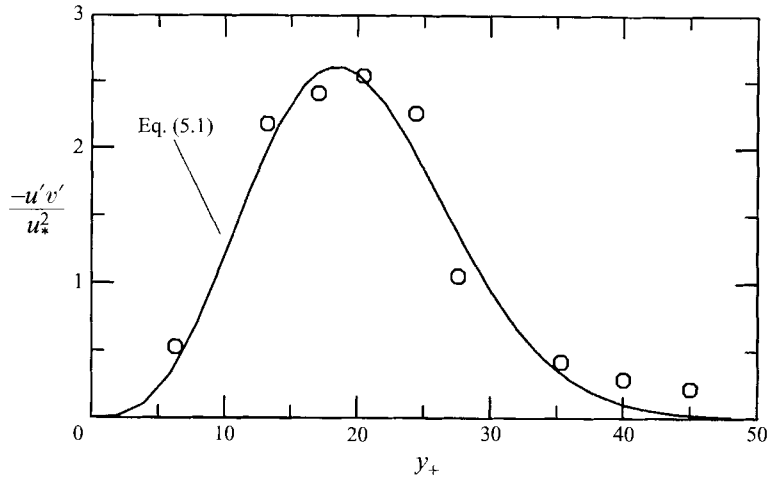

FIGURE 9. Values of the dimensionless Reynolds stress during a bursting ejection event, as predicted by (5.1). Comparison with the experimental data of Kim *et al.* (1971) (circles).

On the other hand, Sumer & Oguz (1978) concluded that ejection events associated with turbulent bursting would be most effective in lifting-up almost neutrally buoyant particles (with values of R of about 0.003 to 0.008) protruding from the viscous sublayer. This is in agreement with the above discussion in that the intensity of the ejection event appears to be higher outside the viscous sublayer (see figure 9). The present results, however, showed that sand particles of sizes larger than the thickness of the viscous sublayer were not entrained into suspension, at least for the range of values of the bed shear stress tested herein, which would indicate that such particles are too heavy to be picked up by such flow ejection events.

5.1.2. *Particle trajectories*

As already discussed, particles appear to be entrained by flow ejection events occurring downstream of convected shear layers. Typical angles of ejection of the particles were observed to be in the range from about 10° to about 20°, which is in good agreement with the values reported by Yung *et al.* (1989). A few trajectories of entrained particles are shown in figure 10, for the experimental conditions d_p = 224 μm, Re = 18 650 and 22 500, and values of Re_{p*} of about 5. As seen therein, some particles are clearly ejected toward the outer regions of the wall layer (values of $y_+ \approx 100$), with an angle of inclination of about 12°, similar to those typical of the shear layers observed in the present experiments. On the other hand some other particles reach maximum elevations corresponding to values of y_+ lower than about 30, after which they tend to fall back toward the bed. From these descriptions it is apparent that the interaction between flow ejections and particles is not always effective in lifting them up to the outer regions of the wall layer. Indeed, although the first group of particles appear to have been trapped in the core of the stretched shear layers and carried along them toward such regions, the second group of particles seem to have fallen from the flow structure in a phenomenon called the crossing-trajectories effect (Wells & Stock 1983; Zhuang, Wilson & Lozowski 1989), thus losing correlation with the fluid motion before the structure loses its coherence.

The latter phenomenon was also observed by Sumer & Deigaard (1981). They carried out experiments with almost neutrally buoyant particles with values of R of

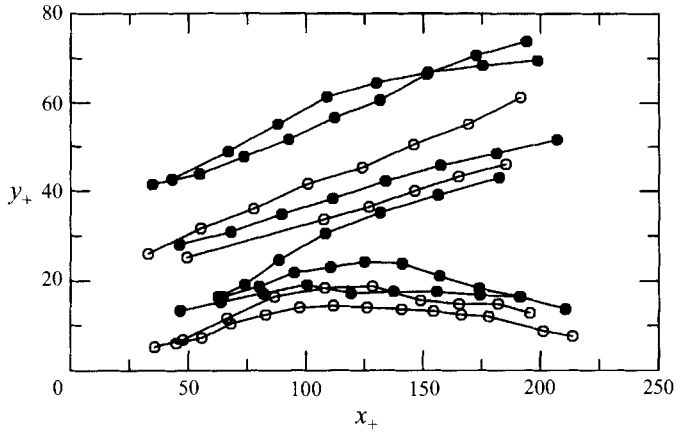

FIGURE 10. Typical trajectories of entrained particles. Experiments of Series S, $d_p = 224$ μm, $Re = 18\,650$ (circles) and 22 500 (solid circles), and values of Re_{p*} of about 5.

about 0.003 to 0.008, and also with slightly heavier particles with values of R of about 0.03, concluding that while the lighter particles follow the flow ejections closely, the heavier ones tend to fall from the flow ejections back to the channel bottom due to the crossing-trajectories effect. In the present experiments, where the particles were much heavier (values of R of about 1.65), both types of behaviour were observed for similar particles, which indicates that the type of path taken by the particle depends on the intensity of the flow ejection event (those events are stochastic in nature, and therefore exhibit variable intensities) and also on the degree of interaction between particle and shear layer reached by the ejected particle, such that more intense events and a high degree of interaction, with the particle trapped in the core of the shear layer, would be associated with particles ejected toward the outer regions of the wall layer, while weaker flow ejection events and a low degree of particle–shear layer interaction would produce premature particle falling from the structure. This argument leads to a slight modification of the conceptual model for the ejections of particles proposed by Sumer & Deigaard (1981), as is shown in figure 11.

With respect to the above point, it was found that the ratio between the number of ejected particles observed to reach the outer region of the wall layer and the total number of ejected particles tends to increase with the dimensionless bed shear stress, τ_*, as shown in figure 12. Therein the experimental points correspond to a value of $d_p = 224$ μm, values of Re in the range from 10 760 to 22 500, and values of Re_{p*} in the range from 4.3 to 5.2, which is relatively narrow and defines particles sizes of the order of the thickness of the viscous sublayer, thus giving them about the same degree of relative exposure to the flow. The results in figure 12 indicate that, on average, the intensity of flow ejection events tends to increase with the bed shear stress, which is in agreement with the results of a VITA analysis of streamwise velocity fluctuations measured near the bed in the present experiments (Niño 1995), which showed that the magnitude of the conditionally averaged velocity fluctuations during ejection events is proportional to u_*. It is also apparent from figure 12 that as the values of τ_* get smaller than about 0.12 a sharp decrease in the effectiveness of flow ejections in lifting particles to the outer regions of the wall layer takes place (Niño & García 1995).

A velocity map of particles being entrained in a particular ejection event corresponding to the experimental conditions $d_p = 112$ μm, $Re = 20\,145$, $Re_{*p} = 2.6$ is

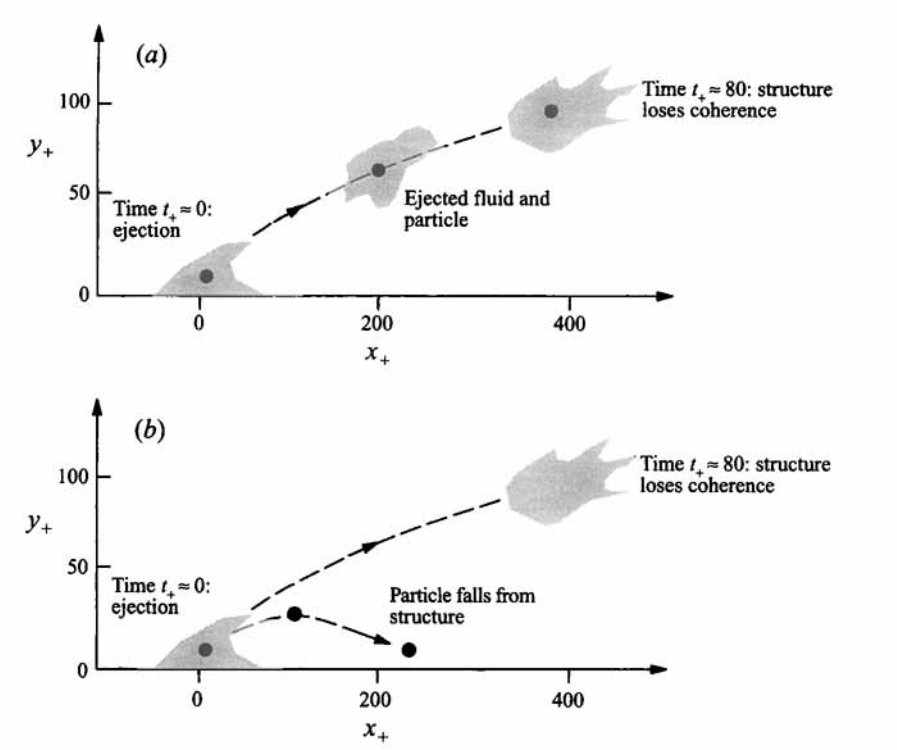

FIGURE 11. Schematic view of particle–flow ejection interactions. (*a*) Case of intense flow ejection event, high degree of particle–shear layer interaction: particle is trapped in the core of the shear layer and ejected to the outer regions of the wall layer until the flow structure loses coherence. (*b*) Case of weak flow ejection event, low degree of particle–shear layer interaction: particle falls from the structure due to the crossing-trajectories effect. Adapted from Sumer & Deigaard (1981).

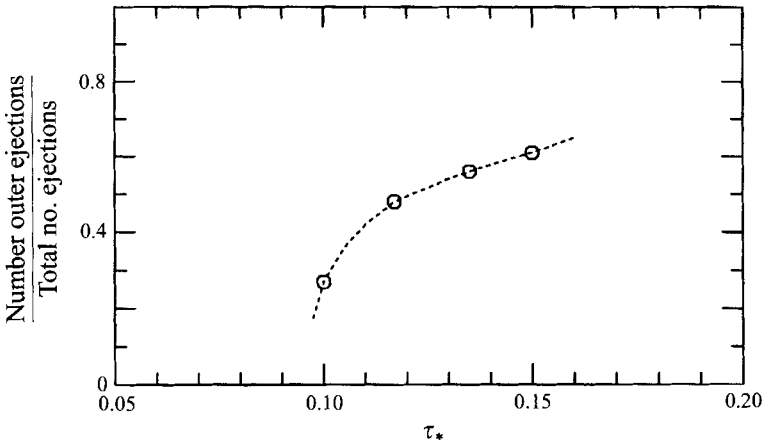

FIGURE 12. Ratio between number of particles ejected to the outer regions of the wall layer and total number of ejected particles as a function of the dimensionless bed shear stress. Experiments of Series S, $d_p = 224$ μm, Re in the range from 10 760 to 22 500, Re_{p*} in the range from 4.3 to 5.2.

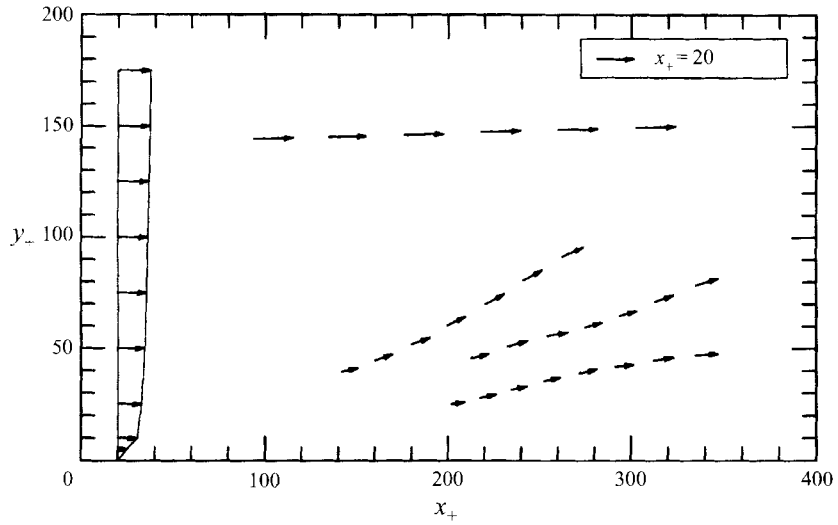

FIGURE 13. Velocity map of suspended particles in one ejection event. Each sequence of arrows corresponds to a different particle. The time interval between arrows of the same sequence corresponds to about 2 wall time units (0.004 s). The velocity profile on the left corresponds to the logarithmic mean velocity profile for smooth flows. Experiments of Series S, $d_p = 112$ μm, $Re = 20\,145$, $Re_{p*} = 2.6$.

shown in figure 13. Therein the sequence of arrows show particle trajectories and the evolution in time of their velocity vector. The time interval between arrows of the same sequence corresponds to 0.004 s. In figure 13, the logarithmic mean velocity profile for smooth flows, given by (Clauser 1956)

$$u_+ = \frac{1}{\kappa} \ln(y_+) + 4.9 \tag{5.2}$$

where κ denotes von Kármán's constant taken as equal to 0.4, is also plotted as a reference. As seen in figure 13, particle trajectories during entrainment are very similar to those shown in figure 10. In this case, two of the three particles being entrained seem to be heading toward the outer regions of the wall layer, while it seems that the third one will not reach heights larger than about 50 wall units. Clearly, the horizontal components of the measured particle velocities during entrainment are considerably lower than the local mean flow velocity predicted by the logarithmic law for smooth flows, which indicates that the streamwise component of the flow velocity fluctuations, u', in the ejection event responsible for the entrainment of the particles has a negative sign. This, added to the obvious fact that the vertical component of such velocity fluctuations, v', is positive during entrainment, shows that the flow ejection event responsible for the entrainment of particles in figure 13 is an event of quadrant 2 ($u' < 0$, $v' > 0$) and thus an important contributor to the Reynolds stress $\overline{u'v'}$, which is in agreement with the results of Kim *et al.* (1971) shown in figure 9. It is also apparent from figure 13 that the magnitude of the particle velocity tends to increase as the particle is lifted-up away from the channel bottom, which is a consequence of the momentum transfer from the flow to the particle, which gets accelerated as it is being dragged by fluid of increasing momentum.

An interesting feature of the situation shown in figure 13 is that there is a fourth particle, which does not seem to be part of the ejection event involving the other

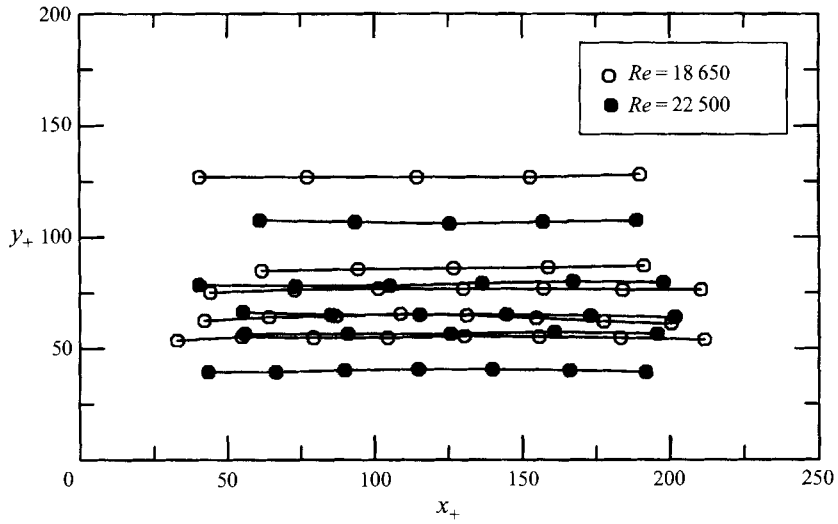

FIGURE 14. Typical trajectories of suspended particles. Experimental conditions as in figure 13.

three particles, and which appears to be moving almost horizontally at a height of about 150 wall units, with a velocity close to that of the local mean flow velocity. Such a particle must have been lifted upto the outer region of the wall layer by a previous ejection event, and kept in suspension by the turbulence of the outer flow. Figure 14 shows a few examples of this situation, where particle trajectories corresponding to the same experimental conditions as those of figure 13 are plotted. As seen therein particles that have been ejected away from the channel bottom can be kept in suspension with trajectories almost parallel to the mean flow velocity for quite long distances, and at elevations as close to the bed as about 40 wall units.

These results indicate that once the particles escape from the lower regions of the wall layer, the turbulence activity prevailing at elevations higher than about 40 wall units somehow induce them to remain suspended for rather long distances before they get deposited back to the bed. Indeed, Browand & Plocher (1985), analysing the entrainment of relatively light particles by the action of turbulent spots in an otherwise laminar flow, concluded that there is a difference between entrainment (the actual lift-up of bed material) and what might be called 'suspendability', which they define as the propensity of particles to remain suspended in a turbulent flow, such that some of the particles they tested, which were never observed to be lifted from the bed by turbulent spots, remained suspended with no difficulty when they were injected in the spots above the wall.

According to their observations of trajectories of almost neutrally buoyant particles, Sumer & Oguz (1978) and Sumer & Deigaard (1981) concluded that the mechanism that keeps particles in suspension would be also related to flow ejections events. They point out that after the particles are lifted-up to the outer regions of the flow by the action of the bursting flow ejections, they tend to fall back to the wall. On the way to the wall the particles are expected to meet fresh lifting fluid due to the next burst from further upstream which will lift them again, or else, in the case where the particles reach the bottom, they would be entrained again by a new flow ejection event. This was also observed by Browand & Plocher (1985), Kaftori *et al.* (1995*a*), and in the present experiments. In fact, in many cases particles that were lifted-up

through their interaction with a shear layer and were lagging that particular structure due to a loss of correlation with it were observed to interact with new developing structures which forced the particles to stay suspended.

It must be pointed out that such a mechanism of particle suspension is plausible within the wall layer; however the flow ejection events that would be responsible for such a mechanism do not extend to the outer flow regions. Therein, different flow coherent structures are suspected to occur, such as the typical eddies (distorted vortex ring-like configurations) and large-scale motions proposed by Falco (1991), which it can be argued, would interact with particles raised to such outer regions by the wall ejection events and keep the particles in suspension, demonstrating on average the process of turbulent diffusion typical of sediment transport in suspension. A typical criterion applied to estimate the conditions required to keep particles in suspension is that of Bagnold (1966), according to which a particle would remain suspended as long as its settling velocity is of lower magnitude than the upward turbulent velocity fluctuations of the flow, a measure of which would be given by the standard deviation of the vertical velocity fluctuations. It has been argued that a further condition required to keep the particle suspended is the asymmetry of the vertical velocity fluctuation time series, such that large positive velocity fluctuations must be more frequent than high negative ones. That is, the skewness of the vertical velocity fluctuations time series must be positive (Bagnold 1966; Wei & Willmarth 1991), which would assure a net upward momentum flux to counteract the effect of gravity on the particle motion. Yen (1992) points out that the fall velocity of a particle in an asymmetric oscillating flow is different from that in still water, such that for certain conditions of frequency, amplitude, and skewness, levitation and hovering against gravitation would be possible. Although there is sufficient evidence that the skewness of the vertical flow velocity fluctuations is indeed positive in wall-bounded turbulent flows, at least outside of the viscous sublayer (Nakagawa & Nezu 1977; Raupach 1981), Wei & Willmarth's (1991) experimental results show negative values of such skewness in the range $10 < y_+ < 30$. As is shown herein, however, this, if true, does not appear to affect the upward transport of sediment from the bed toward the outer regions of the wall layer by bursting ejection events.

It is necessary to add, however, that according to Batchelor (1964) (see also Cermak 1963) particles can diffuse vertically from a local source in a wall boundary layer (which implies the existence of a concentration distribution) just because the effective diffusivity of the turbulence increases in the vertical. This means that the positive skewness condition discussed above may not be necessary to keep a particle in suspension. In fact, particles do not necessarily remain in suspension indefinitely, the equilibrium concentration being constant on average because upward and downward fluxes of particles compensate each other.

5.1.3. *Particle velocities*

Local instantaneous values of the streamwise and vertical components of the particle ejection velocity expressed in wall units, u_{p+} and v_{p+}, respectively, are plotted in figures 15(*a*) and 15(*b*), respectively, as a function of the local value of y_+ where they were measured. Therein each data point corresponds to a different ejected particle, and the values of y_+ correspond to the closest position to the bed available for each case. Experimental conditions are $d_p = 224$ μm, values of Re in the range from 10 760 to 22 500, and values of Re_{p*} in the range from 4.3 to 5.2. In figure 15(*a*), the local mean flow velocity, u_+, given by the law of the wall, $u_+ = y_+$, and the logarithmic velocity profile (5.2), is also plotted as a reference, together with the lines

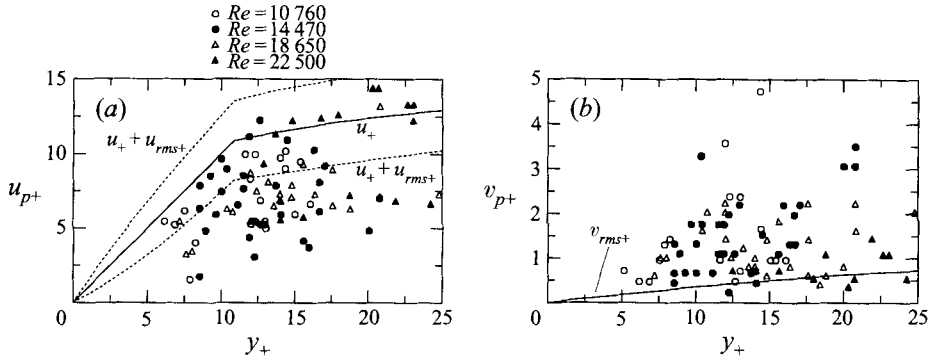

FIGURE 15. Dimensionless local instantaneous values of (*a*) the streamwise component and (*b*) the vertical component of particle ejection velocity. Experiments of Series S, $d_p = 224$ μm, Re in the range from 10760 to 22500, Re_{p*} in the range from 4.3 to 5.2.

defined by $u_+ \pm u_{rms+}$, where u_{rms+} denotes the dimensionless standard deviation of the streamwise flow velocity fluctuations, which was estimated using a best fit of a model proposed by Nezu & Nakagawa (1993) to turbulence measurements made in the present flows, given by

$$u_{rms+} = 2.00 \exp\left(-1.08\frac{y_+}{Re_*}\right)\left(1 - \exp\left(-\frac{y_+}{11.6}\right)\right) + 0.34\, y_+ \exp\left(-\frac{y_+}{11.6}\right) \quad (5.3)$$

where $Re_* = u_* h/\nu$. A value of $Re_* = 900$ was used, which is representative of the range of values of this parameter corresponding to the experimental data shown in figure 15. In figure 15(*b*), the vertical distribution of the dimensionless standard deviation of the vertical component of the flow velocity fluctuations, v_{rms+}, which was estimated using the model proposed by Nakagawa & Nezu (1981), is also plotted as a reference.

As seen in figure 15(*a*), all but a couple of the experimental points have a streamwise ejection velocity smaller than or about equal to the theoretically estimated mean flow velocity, u_+. Furthermore, over about 70% of the experimental points have a streamwise ejection velocity smaller than the theoretically estimated values of the mean flow velocity minus one standard deviation, $u_+ - u_{rms+}$. On the other hand, from figure 15(*b*) it is clear that the observed values of the vertical component of the particle ejection velocity are in general much larger than the local values of the estimated standard deviation of the vertical component of the flow velocity fluctuations, with extreme values of v_{p+} close to about 5. The results presented in figure 15 suggest that the turbulent bursting events responsible for ejecting particles away from the wall would be extreme events of quadrant 2 ($u' < 0$, $v' > 0$) with large values of the flow velocity fluctuations, which is in agreement with the overall discussion about the mechanism for particle entrainment into suspension presented so far.

From the upward trajectories of ejected particles observed in the present experiments, vertical distributions of ensemble-averaged values of the streamwise and vertical components of particle ejection velocity, $\bar{u}_{p+}$ and $\bar{v}_{p+}$, respectively, were computed together with corresponding standard deviations. This was done by dividing the y_+ coordinate in intervals of dimension Δy_+, and ensemble-averaging all the velocity data points (for all the experimental conditions available) contained in each of those intervals. A value $\Delta y_+ = 20$ was used to be consistent with Sumer & Oguz's (1978) analogous analysis. The results obtained are presented

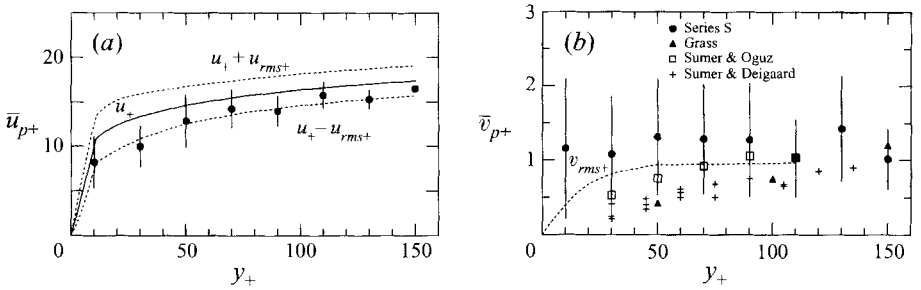

FIGURE 16. Dimensionless ensemble averaged values of (*a*) the streamwise component and (*b*) the vertical component of particle ejection velocity. Experiments of Series S, $d_p = 224$ μm, Re in the range from 10 760 to 22 500, Re_{p*} in the range from 4.3 to 5.2. Symbols denote mean values and vertical lines represent a total length of two standard deviations.

in figures 16(*a*) and 16(*b*). In figure 16(*a*) the results for $\overline{u}_{p+}$ and corresponding standard deviations are plotted as a function of y_+ in the range $0 < y_+ < 150$, together with the mean flow velocity profile given by the law of the wall and the logarithmic profile given by (5.2), and the lines defined by $u_+ \pm u_{rms+}$ as in figure 15(*a*). In figure 16(*b*) the results for $\overline{v}_{p+}$ and corresponding standard deviations are plotted as a function of y_+ in the range $0 < y_+ < 150$, together with the values of v_{rms+} given by the model of Nakagawa & Nezu (1981), and the experimental data by Grass (1974), Sumer & Oguz (1978), and Sumer & Deigaard (1981).

The data by Grass (1974) correspond to average vertical ejection velocities of sand particles with values $d_p = 150$ μm and $Re_{p*} = 4.4$, resulting from the turbulence activity in a boundary layer flow created by towing a flat plate through still water. The data by Sumer & Oguz (1978) and Sumer & Deigaard (1981) correspond to ensemble-averaged vertical components of the velocity of ejected particles in an open channel flow. The particles used by them had rather small values of the submerged specific density, with values of R in the range from 0.003 to 0.03, and values of Re_{p*} in the range from about 30 to about 50.

As seen in figure 16(*a*) the values of $\overline{u}_{p+}$ computed from the present data are generally smaller than the local mean flow velocity, in good agreement with observations by Kaftori *et al.* (1995*b*), and appear to be well described by the curve given by $u_+ - u_{rms+}$. As the particles are lifted to the outer regions of the wall layer they tend to accelerate such that their streamwise velocity gets closer to u_+, which appears to be a consequence of the acceleration of the flow ejection driving the particles due to momentum transfer from the mean flow as it intrudes into regions of high-momentum fluid. It is interesting to note also that the standard deviation of the particle velocity tends to decrease as y_+ increases, and to be of rather small magnitude in the regions outside the wall layer. This is expected since, as pointed out, the flow ejection driving the particles tends to lose coherence as it reaches the outer regions of the wall layer, such that its velocity tends to get close to the mean flow velocity, u_+, with a characteristic standard deviation equal to u_{rms+}, which tends to decrease with y_+ as shown in figure 16(*a*). It is also expected that the values of the standard deviation of the particle velocity be smaller than the values of u_{rms+}, since due to inertial effects the particles tend to filter out high-frequency motions of the driving fluid, thus decreasing the total turbulent energy of the particle motion with respect to that of the flow (Hinze 1971).

As seen in figure 16(*b*), the values of $\bar{v}_{p+}$ computed from the present data tend to be almost constant and equal to about 1.0 to 1.3, with values of the corresponding standard deviation of about 0.5 to 0.9, for values of y_+ in the range from 0 to 150. The values of $\bar{v}_{p+}$ tend to be much larger than the theoretical values of v_{rms+} close to the bed; however they tend to get closer to the latter as the outer regions of the wall layer are approached. It is also apparent from figure 16(*b*) that the values of $\bar{v}_{p+}$ computed from the present data tend to be much larger than the other experimental data presented therein, particularly close to the bed, although such differences decrease substantially as the outer regions of the wall layer are approached.

Of the experimental data plotted in figure 16(*b*), those of Grass correspond to experimental conditions very close to those of the present experiments. However Grass did not provide much detail about his experiments and how the average particle ejection velocities were computed. It is possible, nonetheless, that in his experiments ejection events could have entrained into suspension a larger number of particles than in the present experiments, such that particle–particle interactions could have influenced ejection velocities. On the other hand, the experimental data of Sumer & Oguz and Sumer & Deigaard correspond to particles much larger, albeit less dense, than those used in the present study. The ratio between the particle settling velocity, v_s, and the shear velocity in their experiments was in the range 0.4 to 2.0, very similar to the present range of 1.3 to 1.6. However, the dimensionless time constant, t_{p+}, of their particles was of the order of 100, while that of the present particles is in the range from 2.7 to 4.0. Since t_{p+} is a measure of the inertia of the particles, it is clear that Sumer & Oguz's and Sumer & Deigaard's particles would respond much more slowly to sudden accelerations of the flow than the present particles. In terms of the response to flow ejection events, it can be expected that particles with high values of t_{p+} would have ejection velocities of lower magnitude than that associated with the flow ejections, and would accelerate slowly to match the flow velocity as they are lifted away from the bed. On the other hand particles with low values of t_{p+} would have ejection velocities of magnitude similar to that associated with the flow ejections and would tend to follow the turbulence of the flow rather closely. This would explain the generally low values of the ejection velocities exhibited by Sumer and Oguz's and Sumer and Deigaard's particles in the wall region, as compared to the v_{rms+} values and also to the present experimental results.

From the same upward trajectories of ejected particles analysed to obtain the velocity data presented in figure 16, a correlation between the streamwise and vertical components of the particle ejection velocity was estimated as follows. For each instantaneous particle velocity measured, the dimensionless streamwise and vertical components, u_{p+} and v_{p+}, were computed. The dimensionless particle relative velocity with respect to the mean flow was estimated as $u'_{p+} = u_{p+} - u_+$, $v'_{p+} = v_{p+}$, where u_+ was estimated using the law of the wall and the logarithmic profile (5.2), and the product $(u'_{p+}v'_{p+})$ was computed. Finally, using the same discretization of the vertical coordinate y_+ as previously, with a value $\Delta y_+ = 20$, the ensemble average $\langle u'_{p+}v'_{p+}\rangle$ was computed as a function of y_+. The results obtained are shown in figure 17, plotted together with the experimental data for the Reynolds stress during flow ejection events, $\overline{u'v'}_+$, of Kim *et al.* (1971) shown in figure 9, and the fitted curve (5.1).

As seen in figure 17, the correlation $\langle u'_{p+}v'_{p+}\rangle$ attains a negative peak of about -4.0 close to the wall and then tend to increase toward zero as the outer region of the flow is approached, although the data show large scattering. Clearly the absolute values of $\langle u'_{p+}v'_{p+}\rangle$ during particle ejections are much larger than the absolute values of the

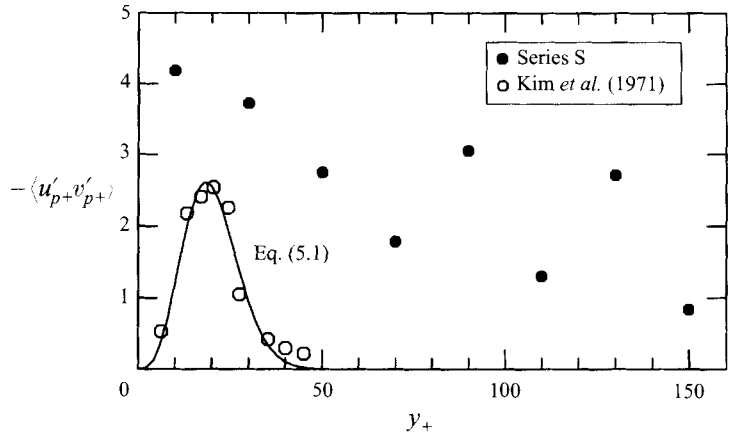

FIGURE 17. Dimensionless correlation between streamwise and vertical components of particle ejection velocity relative to the mean flow velocity. Experiments of Series S, $d_p = 224$ μm, Re in the range from 10 760 to 22 500, Re_{p*} in the range from 4.3 to 5.2.

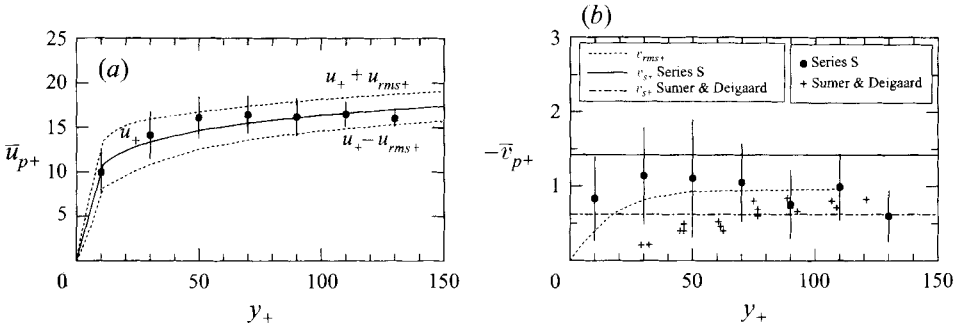

FIGURE 18. Dimensionless ensemble averaged values of (*a*) the streamwise component and (*b*) the vertical component of particle downward velocity. Experiments of Series S, $d_p = 224$ μm, Re in the range from 10 760 to 22 500, Re_{p*} in the range from 4.3 to 5.2. Symbols denote mean values and vertical lines represent a total length of two standard deviations.

Reynolds stress during flow ejection events as measured by Kim *et al.*, which appear to have a maximum of about 3.0 at a distance of about 20 wall units from the bed, and to vanish for values of y_+ larger than 50. There appear to be two issues here. The first is that it is expected that the particles would have a non-zero relative velocity with respect to the driving fluid, which makes the product $\langle u'_{p+}v'_{p+} \rangle$ different from the instantaneous flow value $(u'v')_+$. The second, and perhaps more important, issue is the fact that not every flow ejection event causes the entrainment of particles into suspension, and it can be expected that only the most energetic events would cause such entrainment. Therefore, particles tend to filter out flow ejections having low absolute values of the product $(u'v')_+$, such that the absolute values of the ensemble average $\langle u'_{p+}v'_{p+} \rangle$ would be biased toward values of large magnitude.

The present discussion has concentrated so far on the analysis of particle velocities as they move upward driven by flow ejections; however it is also interesting to analyse particle velocities on their downward path as they fall back to the bed. The results of such an analysis are presented in figure 18(*a*) and 18(*b*). Therein vertical distributions of ensemble-averaged values of the streamwise and vertical components of particle

velocity during downward paths, $\bar{u}_{p+}$ and $\bar{v}_{p+}$, respectively, are plotted together with corresponding standard deviations. In figure 18(*a*), the mean streamwise flow velocity profile given by the law of the wall and the logarithmic law (5.2), and the lines defined by $u_+ \pm u_{rms+}$, with u_{rms+} given by (5.3), are also plotted. In figure 18(*b*), the vertical distribution of v_{rms+} given by the model of Nakagawa & Nezu (1981), the experimental data of Sumer & Deigaard (1981), and lines corresponding to the average dimensionless settling velocity, v_{s+}, of the particles used in the present study and in Sumer & Deigaard's are also plotted for comparison purposes.

As seen in figure 18(*a*) the values of $\bar{u}_{p+}$ computed from the downward trajectories are generally very similar to the values of the theoretical local mean flow velocity, u_+, in good agreement with observations by Kaftori *et al.* (1995*b*), although they tend to be slightly larger in the range of values of y_+ from about 40 to about 70. This is a clear difference with the observed behaviour of the values of $\bar{u}_{p+}$ during ejections which tend to be much smaller than u_+, and is in good agreement with observations by Sumer & Deigaard (1981) who reported larger values of streamwise particle velocities during downward trajectories than during ejections. The corresponding standard deviations of $\bar{u}_{p+}$ for downward trajectories tend to decrease as y_+ increases and to be of smaller magnitude than the values of u_{rms+} of the flow outside the wall layer, similarly to what was observed for ejection trajectories.

Figure 18(*b*) shows that the absolute values of $\bar{v}_{p+}$ for the downward trajectories are somewhat larger than the local values of v_{rms+} for values of y_+ lower than about 70, and that they tend to be about equal to or smaller than such values as the outer region of the wall layer is approached. From figure 18(*b*) is also apparent that the absolute values of $\bar{v}_{p+}$ during downward trajectories are in general only about 60% of the value corresponding to the dimensionless settling velocity of the particles.

It has been argued that relatively light particles would be deposited back to the bed by the action of downward inrushes of high-speed fluid, or sweep events (Cleaver & Yates 1976). Sweep events correspond to highly energetic events of quadrant 4 which would induce streamwise particle velocities larger than the local mean flow velocity, and vertical particle velocities larger than the corresponding settling velocity. It seems from the present observations that the particles are only rarely being deposited by the action of sweep events, and rather they appear on the average to be falling back toward the bed with velocities smaller than the settling velocity as they lose correlation with the turbulent structures that lifted them from the bed and kept them suspended for some time. In fact, the present particle velocity data during downward trajectories Show that only a few extreme events have values of u_{p+} larger than $u_+ + u_{rms+}$, and absolute values of v_{p+} larger than v_{s+}. This is supported also by Sumer & Deigaard's (1981) $\bar{v}_{p+}$ data for downward trajectories, which show that the absolute values of $\bar{v}_{p+}$ tend to be smaller than the corresponding values of v_{s+} in the range of y_+ lower than about 70, although they are similar for larger values of y_+.

The latter conclusion is rather obvious if the following argument is considered. Ejected particles will move upwards as long as the flow vertical velocity component during the ejection is larger than the particle settling velocity. Hence, when the latter exceeds the former in the late ejection stages, the particle will settle back towards the bed with an absolute velocity that is on average less than the particle settling velocity.

5.2. *Experiments of Series T: transitionally rough flows*

5.2.1. *Results from visualizations of flow and particle motion*

Visualizations of particle motion in the near-wall region of the transitionally rough flows of Series T showed that sand particles tend to be lifted away from the bed

by the same ejection mechanism discussed in the previous section for smooth flows, which is in complete agreement with the experimental results for rough flows of Sumer & Deigaard (1981) and Ashida & Fujita (1986). In fact, shear layers with characteristics similar to those observed in the smooth flows of Series S were also commonly observed in the transitionally rough flows of Series T. These structures are seen to maintain their identity for as long as about 60 to 80 wall time units, to extend vertically a distance of about 100 wall units with a mean inclination angle to the bed of about 14°, and to have convection velocities of about 6.5 wall units and frequencies of occurrence of about 0.001 wall units. It is interesting to note that the convection velocity of the structures in the transitional ly rough flows tend to be smaller than that observed in the smooth flows, which indicates that the roughness elements of the bed tend to retard the motion of the shear layers, and which would reflect the fact that the local mean streamwise flow velocity is also retarded by those elements compared to that in the smooth flows. Also, the frequency of occurrence of the shear layers in the transitionally rough flows tends to be about 1/3 of that observed in the smooth flows, which would indicate that the roughness elements have a stabilizing effect on the mechanism that generates flow ejections (Niño 1995).

It must be pointed out that since the particles used in the present experimental study had in general sizes smaller than the roughness elements of the bed, a hiding or sheltering effect was observed which tends to prevent particles from being entrained into suspension by flow ejections. Indeed, as found from an analysis of conditions for the initiation of suspension (Niño & García 1995), as the bed roughness increases (say from smooth to transitionally rough), higher values of the dimensionless bed shear stress τ_* are required to entrain particles of the same size. This hiding effect seems to be dependent on the ratio d_p/d_b, such that as this ratio becomes smaller progressively higher values of τ_* are needed to entrain the particles into suspension, which appears to be related not only to a direct blockage of flow ejections by the roughness elements of the bed so as to preclude the lift of smaller particles, but also to a less local phenomenon involving the modification of the turbulent structure of the flow in the near-bed region. In fact, experimental evidence indicates that near the bed, as the roughness increases, events of quadrant 2 become less important than events of quadrant 4 as contributors to the Reynolds shear stress (Raupach, Antonia & Rajagopalan 1991), which implies a reduction in the ability of the flow to entrain particles into suspension.

5.2.2. *Particle trajectories*

Just as the mechanism of particle entrainment into suspension appears to be common to smooth and rough beds, the trajectories of entrained particles in the transitionally rough flows of Series T are also very similar to those observed in the smooth flows of Series S. The particles are picked up from the bed by flow ejection events, with typical angles of ejection in the range from 10° to about 20°, which is the same as that observed in the experiments of Series S.

A few trajectories of entrained particles are shown in figure 19 for the experimental conditions d_p = 224 μm, Re = 18 840 and 21 480, and values of Re_{p*} of about 7. As seen therein, some particles are ejected toward the outer regions of the wall layer with an angle of inclination of about 14°, similar to those typical of the shear layers observed in the present experiments. On the other hand, some other particles are unable to reach elevations over about 50 wall units from the bed. This latter behaviour, which corresponds to the crossing-trajectories effect discussed previously, is also totally analogous to that observed for the smooth flows.

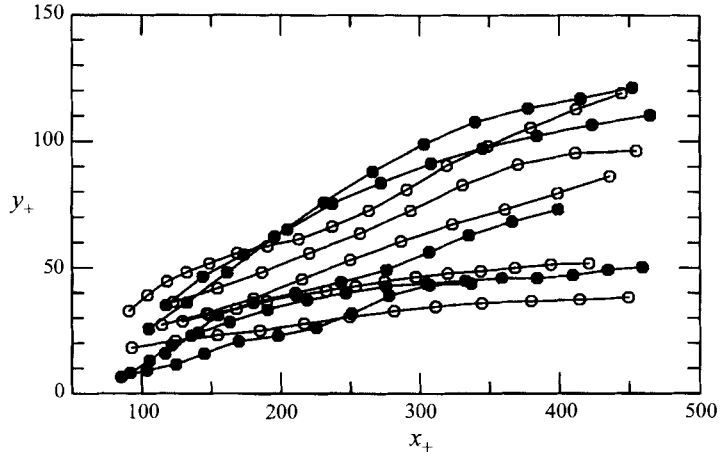

FIGURE 19. Typical trajectories of entrained particles. Experiments of Series T, $d_p = 224$ μm, $Re = 18\,840$ (circles) and 21 480 (solid circles), and values of Re_{p*} of about 7.

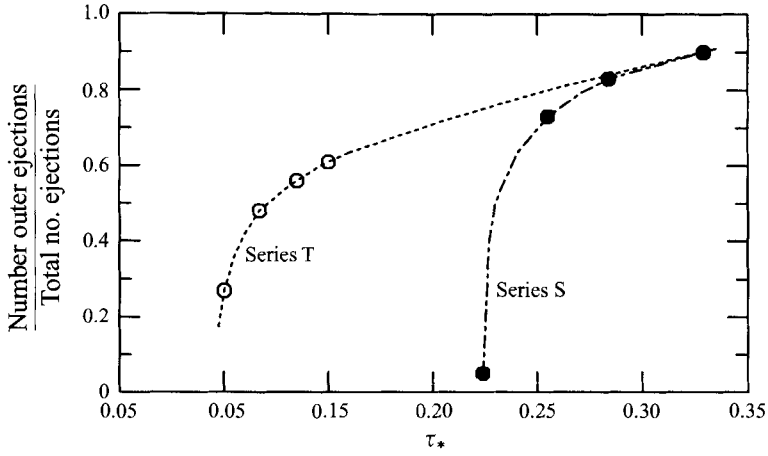

FIGURE 20. Ratio of number of particles ejected to the outer regions of the wall layer to total number of ejected particles as a function of the dimensionless bed shear stress. Experiments of Series T correspond to $d_p = 224$ μm, Re in the range from 16 360 to 25 240, Re_{p*} in the range from 6.4 to 7.7. Experiments of Series S correspond to the same conditions as those of figure 12.

An apparent difference in the behaviour of the entrained particles in the transitionally rough flows with respect to those observed in the smooth flows was that on average the former tended to reach higher elevations than the latter. In fact, it seems that in those experiments with transitionally rough flows, relatively more particles were able to reach the outer regions of the wall layer than in the case of smooth flows. However, as is explained below, this is a consequence of the larger values of the dimensionless bed shear stress used in the rough case.

In figure 20, the ratio of the number of ejected particles observed to reach the outer region of the wall layer to the total number of ejected particles is plotted as a function of the dimensionless bed shear stress, τ_*, for the experiments of Series T corresponding to a value of $d_p = 224$ μm, values of Re in the range from 16 360 to 25 240, and values of Re_{p*} in the range from 6.4 to 7.7. In the same figure equivalent

results for the experiments of Series S presented previously in figure 12 are also plotted for comparison.

As seen in figure 20, it is apparent that for values of τ_* lower than about 0.22 no particles are ejected to the outer region of the wall layer in the transitionally rough flows, contrary to what was observed in the case of smooth flows. This is related to the hiding effect discussed previously (for details see Niño & García 1995). For values of τ_* larger than about 0.28 the ratio of the number of outer ejections to the total number of ejections for the transitionally rough flows is larger than 0.8, and it can be speculated that it tends asymptotically to a curve extrapolated from the results corresponding to the smooth flows in the range of values of τ_* lower than 0.15.

The results shown in figure 20 clearly demonstrate that, on average, fewer particles were able to reach the outer regions of the wall layer in the experiments of Series S than for Series T, simply because the intensity of the flow ejection events responsible for the entrainment of particles (which as concluded from (5.1) is positively correlated with τ_*) in the former case was lower than in the latter.

5.2.3. *Particle velocities*

From the upward trajectories of ejected particles observed in the experiments of Series T, vertical distributions of ensemble-averaged values of the streamwise and vertical components of particle ejection velocity, $\bar{u}_{p+}$ and $\bar{v}_{p+}$, respectively, were computed together with corresponding standard deviations. This was done by discretizing the y_+ coordinate in the same way as it was done previously for the results shown in figure 16. The results obtained are presented in figure 21(*a*) and 21(*b*). In figure 21(*a*) the results for $\bar{u}_{p+}$ and corresponding standard deviations are plotted as a function of y_+ in the range $0 < y_+ < 150$, together with the distribution of u_+ given by the logarithmic velocity profile valid for transitionally rough flows (Schlichting 1968):

$$u_+ = \frac{1}{\kappa} \ln\left(\frac{y_+}{k_{s+}}\right) + B \tag{5.4}$$

where k_{s+} corresponds to the bed roughness size made dimensionless with wall units and B is a parameter which is a function of k_{s+}. In figure 21(*a*) the lines defined by $u_+ \pm u_{rms+}$ are also plotted, similarly as in figure 16(*a*), where u_{rms+} was estimated using the relation (5.3) valid for smooth flows. A value $k_{s+} = 32.3$ was used in (5.4) together with its associated value $B = 9.1$, while a value $Re_* = 1665$ was used in (5.3), which are representative of the range of values of these parameters corresponding to the experimental data shown in figure 21. In figure 21(*b*), the results for $\bar{v}_{p+}$ and corresponding standard deviations are plotted as a function of y_+ also in the range $0 < y_+ < 150$, together with the distribution of v_{rms+} for smooth flows, similarly as in figure 16(*b*), the data of Grass (1971), the data of Sumer & Deigaard (1981) corresponding to rough flows, and the results obtained in Series S and presented previously in figure 16(*b*), for comparison.

As seen in figure 21(*a*), the values of $\bar{u}_{p+}$ computed from the data of Series T are generally smaller than the theoretical local mean flow velocity, and appear to be well described by the curve given by $u_+ - u_{rms+}$, which implies a behaviour completely analogous to that observed in the smooth flows experiments. Nevertheless, there is a tendency for the closest point to the bed to have a velocity somewhat larger than $u_+ - u_{rms+}$, which can be explained by pointing out that the values of u_{rms+} plotted in figure 21(*a*) are those corresponding to smooth flows, which are known to be larger than those associated with rough flows close to the bottom wall, although both of them become similar as y_+ increases over about 60 (Nezu & Nakagawa

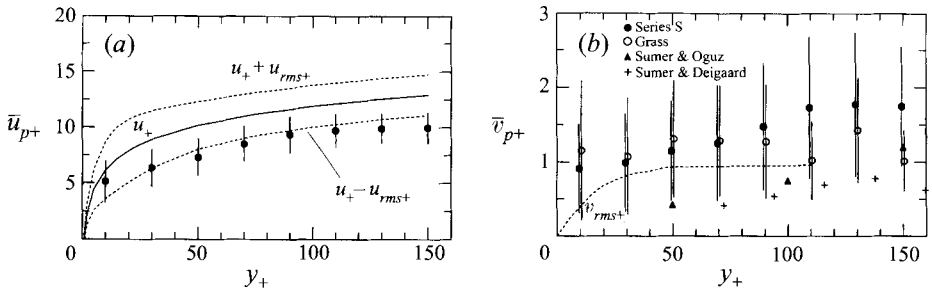

FIGURE 21. Dimensionless ensemble averaged values of (*a*) the streamwise component and (*b*) the vertical component of particle ejection velocity. Experiments of Series T, $d_p = 224$ μm, Re in the range from 18 840 to 25 240, Re_{p*} in the range from 6.8 to 7.7. Symbols denote mean values and vertical lines represent a total length of two standard deviations.

1993). From figure 21(*a*) is also apparent that standard deviations corresponding to the values of $\overline{u}_{p+}$ tend to decrease as y_+ increases, similarly to u_{rms+}, and to be of smaller magnitude, which is expected because of particle inertial effects as discussed previously. This behaviour of the standard deviation of $\overline{u}_{p+}$ is also analogous to that observed in the case of smooth flows.

In figure 21(*b*), the values of $\overline{v}_{p+}$ computed from the data of Series T show some tendency to increase as y_+ increases, from values close to about 1.0 near the bottom wall to values close to about 2.0 in the regions outside the wall layer, with corresponding values of the standard deviation of about 0.5 to 0.9. As in the smooth flow case, the values of $\overline{v}_{p+}$ seem to be always larger than the theoretically estimated values of v_{rms+}, at least in the range $0 < y_+ < 150$. As seen in figure 21(*b*), the $\overline{v}_{p+}$ values are very similar to those estimated in the smooth flow case except for y_+ larger than about 100, for which the values of $\overline{u}_{p+}$ of Series T tend to be larger than those of Series S. This behaviour suggests that the flow ejections in a rough bed would be more intense than those in a smooth flow, which is in agreement with the observations of Sumer & Deigaard (1981) who also reported somewhat larger particle vertical ejection velocities in the case of rough flows than in the case of smooth flows. Grass (1971) concluded from his observations that although the flow ejection mechanism would be much the same over a rough bed as over a smooth surface, flow entrainment tends to be much more violent in the rough bottom case. Nevertheless, as pointed out by Sumer & Deigaard (1981), this enhanced intensity does not appear to influence much the behaviour of particles entrained from the rough bed, which does not seem to differ appreciably from that corresponding to the smooth surface case.

From figure 21(*b*), it is also apparent that the values of $\overline{v}_{p+}$ computed from the data of Series T tend to be much larger than the experimental values of this variable reported by Grass (1974) and Sumer & Deigaard (1981), the latter corresponding to their experiments over a rough bed. It is also apparent that their estimated values of $\overline{v}_{p+}$ are smaller than the values of v_{rms+}, which somehow contradicts the notion of having particularly strong events of quadrant 2 driving the particle ejections from the bed. As indicated previously, there is insufficient information available about Grass' experiments to explain the apparent differences with the present observations. However, as mentioned earlier, particle–particle interaction could have been an important factor. On the other hand, the differences between the present experimental results and those of Sumer & Deigaard can be again explained in terms of the different values of the dimensionless particle time constant, t_{p+}. In

fact, the values of t_{p+} in Sumer & Deigaard's rough bed experiments were about 240, much larger than those in the present experiments of Series T, which were only about 7 to 9. Since t_{p+} is a measure of the inertia of the particles, it is clear that Sumer & Deigaard's particles would respond much more slowly to sudden accelerations of the flow, such as those associated with flow ejection events, than those of Series T, which would imply smaller vertical ejection velocities in the former case than in the latter. This conclusion is analogous to that given to explain equivalent differences observed in the case of smooth flows.

6. Conclusions

The evidence presented herein indicates that wall streaks in a smooth channel flow are related to the presence of counter-rotating quasi-streamwise vortices. These extend about 1000 to 2000 wall units in the streamwise direction, and about 15 to 25 wall units in the vertical direction, persist on average for about 500 wall time units and have a transverse wavelength of about 100 wall units. Groups of 3 to 5 counter-rotating pairs of such vortices emerge and collapse quasi-periodically in time, and are distributed rather randomly along the bottom wall. These vortices induce particle sorting along low-speed streaks when the particles are of sizes about equal or smaller than the thickness of the viscous sublayer. Larger particles do not tend to accumulate along wall streaks; however they respond to the near-bed flow velocity streaky pattern by moving faster when they are located in high-speed regions. The presence of particles of sizes about equal to or smaller than the thickness of the viscous sublayer does not affect the wavelength of the wall streaks; however it somehow stabilizes these flow structures, such that they have durations about 2 to 3 times longer than those observed in the absence of particles.

In the case of a rough boundary, the roughness elements disrupt the structure of the viscous sublayer, and although the wall streaks also develop in these conditions, they lose coherence, persistence, and spatial extent. Particles of sizes smaller than about 1/5 of the size of the roughness elements move within the interstices of them without sorting along any preferential paths. Larger particles move over the roughness elements; however they do not respond to the sorting effect of the rather weak wall streaks.

Low-momentum fluid is lifted-up from the bed as a consequence of quasi-periodic ejection events and evolves into some kind of coherent structure. This mechanism appears to be common to the flow over both smooth and rough surfaces. The most frequently observed coherent structures correspond to shear layers of concentrated spanwise vorticity, which have a typical inclination angle to the bed of about 14°. Apparently, an intense flow ejection (event of quadrant 2) occurs downstream from the shear layer, at a distance of about 100 to 200 wall units.

Particles are picked up from the bed by flow ejection events occurring downstream of the shear layers. Particle ejection angles are in the range 10° to 20°, very similar to the angle of inclination of the shear layers. After the particles are lifted from the bed their relative motion is toward the shear layer so they eventually interact more directly with the flow structures. Particles trapped in the core of the shear layers are raised toward the outer regions of the wall layer as the flow structure is stretched out into such regions. After the shear layers lose coherence the particles tend to fall back to the bed, although in some cases they are maintained in suspension for rather long period of time by some other coherent motions developing in the outer region of the wall layer. In their path back to the wall the particles can

either be deposited or picked up by a new developing ejection event and returned to the outer regions of the wall layer. A second type of interaction occurs when the particle lags the shear layer, eventually falling from the structure back to the bed, without reaching elevations higher than about 50 wall units (the crossing-trajectories effect).

The number of particles reaching the outer regions of the wall layer increases with the dimensionless bed shear stress, τ_*, which would indicate that the intensity of the flow ejections responsible for the particle entrainment into suspension also increases with this variable. In the case of transitionally rough flows, a hiding effect was observed, which tended to preclude particles from being entrained into suspension at values of τ_* for which such entrainment was observed in the case of smooth flows.

Measured instantaneous particle velocities during ejections in both smooth and transitionally rough flows show that their streamwise component tends to be much lower than the local mean flow velocity, while their vertical component tends to be rather intense, much larger than the local standard deviation of the vertical flow velocity fluctuations, which would indicate that such particles are responding to rather extreme flow events of quadrant 2. Dimensionless ensemble-averaged values of the streamwise component of particle velocity during ejections, $\bar{u}_{p+}$, measured in both the smooth and transitionally rough flows are well described by a theoretical line given by $u_+ - u_{rms+}$. On the other hand, in the case of smooth flows, dimensionless ensemble-averaged values of the vertical component of the particle velocity during ejections, $\bar{v}_{p+}$, tend to be approximately constant in the range $0 < y_+ < 150$, with values of about 1.0 to 1.5 wall units. These values are much larger than v_{rms+} close to the bed, and similar to this variable in the outer region of the wall layer. In the case of the transitionally rough flows, values of $\bar{v}_{p+}$ during ejections are very similar to those observed in the smooth flows, except at values of y_+ larger than about 100 where they tend to be larger than them, reaching values of about 2.0 wall units. This would indicate that flow ejections in the transitionally rough flows would be more intense than those in the smooth flows, in agreement with previous observations. Values of $\bar{v}_{p+}$ measured herein are much larger than those of previous experiments; however the differences could be explained in terms of the dimensionless particle time constant, t_{p+}, which is much smaller in the present experiments, indicating a much faster response of the present particles to sudden accelerations of the flow.

The analysis of the particle velocity during downward trajectories shows that values of the dimensionless ensemble-averaged streamwise component of the particle velocity are about the same magnitude as the local mean flow velocity, while corresponding values of the dimensionless ensemble-averaged vertical component of the particle velocity tend to be somewhat smaller in absolute value than the particle dimensionless settling velocity, although larger than v_{rms+}. These results suggest that particles would be only rarely deposited by the action of sweep events, but rather they appear to be falling back toward the bed as they lose correlation with the turbulent structures that lifted them from the bed and kept them suspended for some time.

Finally, it should be stressed that the present conclusions are valid at least within the present range of values of relevant dimensionless parameters used in the study. For example, the flow Reynolds number, which in the present experiments was lower than about 30 000, has an important influence on the characteristics of turbulent coherent structures, and thus on the phenomenon of particle entrainment into suspension. It is a matter of further study to verify that the conclusions obtained herein remain valid at larger values of the flow Reynolds number.

We would like to give special thanks to Fabián López for his help with the experimental study and his contribution to discussions presented in this paper. We also thank the National Science Foundation (grant CTS–9210211), the Office of Naval Research (grant N00014–93–1–0044), and the donors of the Petroleum Research Fund, administered by the American Chemical Society (grant PRF 24328–G2) for supporting this research. Finally, we would like to thank anonymous reviewers for their valuable suggestions and comments.

REFERENCES

ASHIDA, K. & FUJITA, M. 1986 Stochastic model for particle suspension in open channels. *J. Hydrosci. Hydr. Engng* **4**, 21–46.

BAGNOLD, R. A. 1966 An approach to the sediment transport problem for general physics. *Geological Survey Professional Paper* 422–I, Washington, DC.

BARK, F. 1975 On the wave structure of the wall region of a turbulent boundary layer. *J. Fluid Mech.* **70**, 229–250.

BATCHELOR, G. K. 1964 Diffusion from sources in a turbulent boundary layer. In *Arch. Mech. Stosowanej* **3**(16), 661–670.

BEST, J. 1992 On the entrainment of sediment and initiation of bed defects: insights from recents developments within turbulent boundary layer research. *Sedimentology* **39**, 797–811.

BLACKWELDER, R. F. 1988 Coherent structures associated with turbulent transport. In *Transport Phenomena in Turbulent Flows: Theory, Experiments, and Numerical Simulation* (ed. M. Hirata & N. Kasagi), pp. 69–88.

BROWAND, F. K. & PLOCHER, D. A. 1985 Image processing for sediment transport. In *Proc. 21st Congress IAHR, Melbourne, Australia*, pp. 8–14.

CERMAK, J. E. 1963 Lagrangian similarity hypothesis applied to diffusion in turbulent shear flow. *J. Fluid Mech.* **15**, 49–63.

CLAUSER, F. H. 1956 The turbulent boundary layer. *Adv. Appl. Mech.* **4**, 1–31.

CLEAVER, J. W. & YATES, B. 1976 The effect of re-entrainment on particle deposition. *Chem. Engng Sci.* **31**, 147–151.

DILL, A. J. 1994 Video-based particle tracking velocimetry technique for measuring flow velocity in porous media. Masters Thesis, Dept. Civil Engng. Univ. of Illinois at Urbana-Champaign, Illinois.

FALCO, R. E. 1991 A coherent structure model of the turbulent boundary layer and its ability to predict Reynolds number dependence. *Phil. Trans. R. Soc. Lond.* A **336**, 103–129.

GARCÍA, M., LÓPEZ, F. & NIÑO, Y. 1995 Characterization of near-bed coherent structures in open channel flow using synchronized high-speed video and hot-film measurements. *Exps. Fluids* **19**, 16–28.

GRASS, A. J. 1974 Transport of fine sand on a flat bed: turbulence and suspension mechanics. In *Euromech* 48, pp. 33–34. Inst. Hydrodynamic and Hydraulic Engrg. Tech. Univ. Denmark.

GRASS, A. J. 1971 Structural features of turbulent flow over smooth and rough boundaries. *J. Fluid Mech.* **50**, 233–255.

GRASS, A. J., STUART, R. J. & MANSOUR-TEHRANI, M. 1991 Vortical structures and coherent motion in turbulent flow over smooth and rough boundaries. *Phil. Trans. R. Soc. Lond.* A **336**, 35–65.

GUEZENNEC, Y. G., PIOMELLI, U. & KIM, J. 1989 On the shape and dynamics of wall structures in turbulent channel flow. *Phys. Fluids* A **1**, 764–766.

HASSAN, Y. A., BLANCHAT, T. K., SEELEY, C. H. & CANAAN, R. E. 1992 Simultaneous velocity measurements of both components of a two-phase flow using Particle Image Velocimetry. *Intl J. Multiphase Flow* **18**, 371–395.

HETSRONI, G. 1991 The effect of particles on the turbulence in a boundary layer. In *Two Phase Flow* (ed. M. Rocco), Chap. 8. Butterworth.

HINZE, J. O. 1971 Turbulent fluid and particle interaction. *Progress Heat Mass Transfer* **6**, 433–452.

JACKSON, R. G. 1976 Sedimentological and fluid dynamics implications of the turbulent bursting phenomenon in geophysical flows. *J. Fluid Mech.* **77**, 531–560.

JIMENEZ, J., MOIN, P., MOSER, R. & KEEFE, L. 1988 Ejection mechanisms in the sublayer of a turbulent channel. *Phys. Fluids* **31**, 1311–1313.

KAFTORI, D., HETSRONI, G. & BANERJEE, S. 1995*a* Particle behaviour in the turbulent boundary layer I. Motion, deposition, and entrainment. *Phys. Fluids* **7**, 1095–1106.

KAFTORI, D., HETSRONI, G. & BANERJEE, S. 1995*b* Particle behaviour in the turbulent boundary layer II. Velocity and distribution profiles. *Phys. Fluids* **7** 1107 –1121.

KIM, H. T., KLINE, S. J. & REYNOLDS, W. C. 1971 The production of turbulence near a smooth wall in a turbulent boundary layer. *J. Fluid Mech.* **50**, 133–160.

KLINE, S. J., REYNOLDS, W. C., SCHRAUB, F. A. & RUNSTADLER, P. W. 1967 The structure of turbulent boundary layers. *J. Fluid Mech.* **30**, 741–773.

LIU, Z., LANDRETH, C. C., ADRIAN, R. J. & HANRATTY, T. J. 1991 Measurements in turbulent channel flow by high resolution Particle Image Velocimetry. *Exps. Fluids* **10**, 301–312.

MOIN, P. & KIM, J. 1982 Numerical investigation of turbulent channel flow. *J. Fluid Mech*, **118**, 341–377.

MOIN, P. & SPALART, P. R. 1989 Contributions of numerical simulation data bases to the physics, modelling, and measurement of turbulence. In *Advances in Turbulence* (ed. W. K. George & R. Arndt), pp. 11–38. Hemisphere/Springer.

NAKAGAWA, H. & NEZU, I. 1977 Prediction of the contributions to the Reynolds stress from bursting events in open-channel flows. *J. Fluid Mech.* **80**, 99–128.

NAKAGAWA, H. & NEZU, I. 1981 Structure of space–time correlations of bursting phenomena in an open-channel flow. *J. Fluid Mech.* **104**, 1–43.

NEZU, I. & NAKAGAWA, H. 1993 Turbulence in open-channel flows. In *IAHR Monograph*. A. A. Balkema, Rotterdam.

NIÑO, Y. 1995 Particle motion in the near-wall region of a turbulent open channel flow: implications for bedload transport by saltation and sediment entrainment into suspension. PhD Thesis. University of Illinois at Urbana-Champaign. Urbana, Illinois.

NIÑO, Y. & GARCÍA, M. 1995 Threshold for particle entrainment into suspension. *J. Hydraul. Engng ASCE* (submitted).

PEDINOTTI, S., MARIOTTI, G. & BANERJEE, S. 1992 Direct numerical simulation of particle behaviour in the wall region of turbulent flows in horizontal channels. *Intl J. Multiphase Flow* **18**, 927–941.

PERRY, A. E. & LI, J. D. 1990 Experimental support for the attached-eddy hypothesis in zero-pressure-gradient turbulent boundary layers. *J. Fluid Mech.* **218**, 405–438.

PERRY, A. E., SCHOFIELD, W. H. & JOUBERT, P. N. 1969 Rough wall turbulent boundary layers. *J. Fluid Mech.* **37**, 383–413.

RASHIDI, M., HETSRONI, G. & BANERJEE, S. 1990 Particle-turbulence interaction in a boundary layer. *Intl J. Multiphase Flow* **16**, 935–949.

RAUPACH, M. R. 1981 Conditional statistics of Reynolds stress in rough-wall and smooth-wall turbulent boundary layers. *J. Fluid Mech.* **108**, 363–382.

RAUPACH, M. R., ANTONIA, R. A. & RAJAGOPALAN, S. 1991 Rough-wall turbulent boundary layers. *Appl. Mech. Rev.* **44**, No. 1.

ROBINSON, S. K. 1990 Kinematics of turbulent boundary layer structure. PhD dissertation. Standford University.

ROBINSON, S. K. 1991 Coherent motions in the turbulent boundary layer. *Ann. Rev. Fluid Mech.* **23**, 601–639.

SCHLICHTING, H. 1968 *Boundary-Layer Theory*. McGraw–Hill.

SCHMID, A. 1985 Wandnahe turbulente bewegungsabläufe und ihre bedeutung für die riffelbildung. *Institute für Hydromechanik und Wasserwirtschaft*, R 22–85. ETH, Zürich.

SMITH, C. R. & SCHWARTZ, S. P. 1983 Observation of streamwise rotation in the near-wall region of a turbulent boundary layer. *Phys. Fluids* **26** 641–652.

SUMER, B. M. & DEIGAARD, R. 1981 Particle motions near the bottom in turbulent flow in an open channel. Part 2. *J. Fluid Mech.* **109**, 311–337.

SUMER, B. M. & OGUZ, B. 1978 Particle motions near the bottom in turbulent flow in an open channel. *J. Fluid Mech.* **86**, 109–127.

SUTHERLAND, A. J. 1967 Proposed mechanism for sediment entrainment by turbulent flows. *J. Geophys. Res.* **72**, 191–198.

URUSHIHARA, T., MEINHART, C. D. & ADRIAN, R. J. 1993 Investigation of the logarithmic layer in pipe flow using Particle Image Velocimetry. In *Near-Wall Turbulent Flows* (ed. R. M. C. So, C. G. Speziale & B. E. Launder). Elsevier.

WEI, T. & WILLMARTH, W. 1991 Examination of v-velocity fluctuations in a turbulent channel flow in the context of sediment transport. *J. Fluid Mech.* **233**, 241–252.

WELLS, M. R. & STOCK, D. E. 1983 The effects of crossing trajectories on the dispersion of particles in a turbulent flow. *J. Fluid Mech.* **136**, 31–62.

YEN, B. C. 1992 Sediment fall velocity in oscillating flow. *Water Resour. and Environ. Engrg. Res.*, Rep. 11. Dept. of Civil Engng. University of Virginia.

YUNG, B. P. K., MERRY, H. & BOTT, T. R. 1988 The role of turbulent bursts in particle re-entrainment in aqueous systems. *Chem. Engng Sci.* **44**, 873–882.

ZHUANG, Y., WILSON, J. D. & LOZOWSKI, E. P. 1989 A trajectory-simulation model for heavy particle motion in turbulent flow. *J. Fluids Engng* **111**, 492–494.